

RSC Applied Interfaces

Accepted Manuscript

This article can be cited before page numbers have been issued, to do this please use: D. M. Cox-Pridmore, E. Mishra, M. A. Webber and S. Qi, *RSC Appl. Interfaces*, 2026, DOI: 10.1039/D6LF00022C.



This is an Accepted Manuscript, which has been through the Royal Society of Chemistry peer review process and has been accepted for publication.

Accepted Manuscripts are published online shortly after acceptance, before technical editing, formatting and proof reading. Using this free service, authors can make their results available to the community, in citable form, before we publish the edited article. We will replace this Accepted Manuscript with the edited and formatted Advance Article as soon as it is available.

You can find more information about Accepted Manuscripts in the [Information for Authors](#).

Please note that technical editing may introduce minor changes to the text and/or graphics, which may alter content. The journal's standard [Terms & Conditions](#) and the [Ethical guidelines](#) still apply. In no event shall the Royal Society of Chemistry be held responsible for any errors or omissions in this Accepted Manuscript or any consequences arising from the use of any information it contains.

Data Availability Statement

View Article Online
DOI: 10.1039/D6LF00022C

All data supporting the findings of this study are contained within the article. This includes both original data generated in the course of the research and previously published data cited in the references.



Antibacterial Surface Engineering: Bioinspiration from Leaves to Medical Devices

View Article Online
DOI: 10.1039/D6LF00022C

Danielle M. Cox-Pridmore^{1,2,3}, Eleanor Mishra^{3,4,5}, Mark Webber^{2,3}, Sheng Qi^{1,3,6*}

1 School of Chemistry, Pharmacy and Pharmacology, Faculty of Science, University of East Anglia, Norwich Research Park, Norwich, NR4 7TJ

2 Quadram Institute, Rosalind Franklin Road, Norwich Research Park, NR4 7UQ

3 Centre for Microbial Interactions, Norwich Research Park, Norwich NR4 7UG, United Kingdom

4 Department of Respiratory Medicine, Norfolk & Norwich University Hospital, Norwich, NR4 7UY

5 Faculty of Medicine & Health Sciences, University of East Anglia, Norwich Research Park, Norwich, NR4 7TJ

6 School of Pharmacy and Pharmaceutical Sciences, Institute of Systems, Molecular and Integrative Biology, University of Liverpool, Liverpool, L69 3GE

Corresponding author*: sheng.qi@liverpool.ac.uk



26 Abstract

27 Healthcare-acquired infections (HAIs) and the rise of antimicrobial resistance (AMR) are
28 critical global health challenges, necessitating innovative solutions to combat pathogenic
29 bacteria. Traditional approaches, such as antibiotics and chemical disinfectants, are
30 increasingly ineffective due to the rapid evolution of resistant strains and their associated side
31 effects and environmental impacts. The development of antimicrobial physical surface design
32 strategies presents a promising alternative for reducing microbial colonisation and
33 transmission.

34 This review provides a comprehensive examination of antimicrobial surface geometries and
35 topographies, focusing on physical surface strategies that prevent bacterial adhesion and
36 biofilm formation. Inspired by naturally occurring structures such as insect wings and lotus
37 leaves, these engineered surfaces employ nano- and micro-scale patterning to exert mechanical
38 forces that disrupt microbial cells through membrane rupture or inhibit their attachment by
39 limiting surface area for successful adhesion. We discuss key fabrication methods, mechanisms
40 of action, material considerations, and clinical relevance, while also addressing challenges such
41 as scalability, durability, and regulatory issues.

42 By highlighting both the potential and limitations of physical surface modifications in
43 healthcare environments, this review aims to inform future research and promote the
44 integration of surface-based strategies in the design of next-generation medical devices and
45 high-touch clinical surfaces.

47 **Keywords:** Antimicrobial surfaces, surface topography, healthcare-acquired infections,
48 biofilms, antimicrobial resistance, medical devices.

49



50 1. Introduction

View Article Online
DOI: 10.1039/D6LF00022C

51 1.1. Bacterial Biofilms and Infection

52 Bacteria are a family of single-cell microorganisms that play a crucial role in a wide array of
53 biological processes, environmental cycles, and technological applications. Their remarkable
54 ability to adapt to various environments, coupled with their metabolic diversity, makes them
55 essential for maintaining ecological balance and supporting life on Earth. However, some
56 bacteria are pathogenic, resulting in harmful infections, and therefore, are a major focus of
57 medical research and public health efforts¹⁻³.

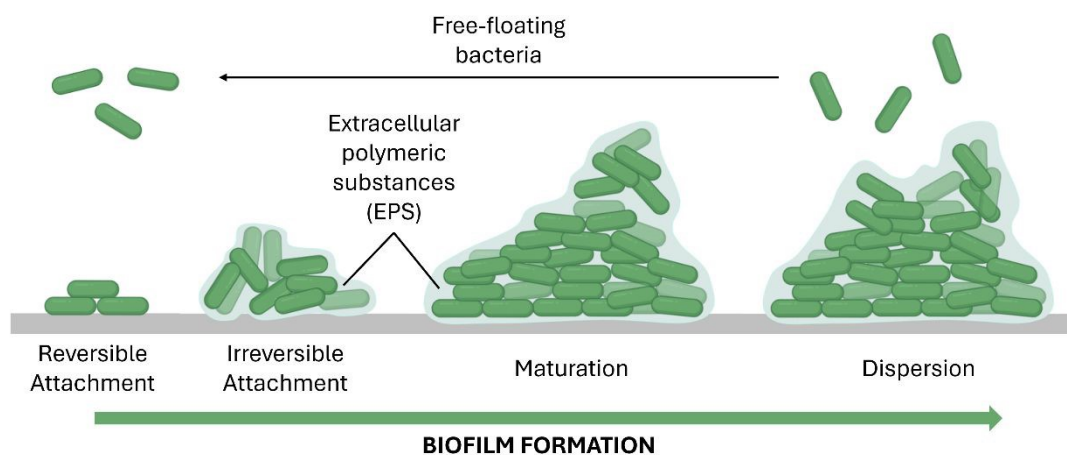
58 It is well established that bacteria can efficiently colonise surfaces and form a biofilm rather
59 than dwelling in a planktonic state^{4,5}, with current estimates suggesting that up to 80% of
60 bacteria reside in biofilms⁶. A biofilm (**Figure 1**) is a complex, structured community of
61 bacteria encased in a self-produced matrix of extracellular polymeric substances (EPS),
62 composed of polysaccharides, proteins, and nucleic acids⁷, that adhere to living or inert
63 surfaces such as medical devices, for example, catheters, implants, and prosthetics⁸⁻¹⁰.

64 Biofilm formation is a dynamic, multistage process that begins with the reversible attachment
65 of planktonic (free-floating) microorganisms to the surface. This transitions to irreversible
66 attachment, and bacteria begin to secrete EPS, forming a matrix that encases the cells and
67 anchors them to the surface. As the biofilm grows and matures, microbial cells communicate
68 with each other through quorum sensing to coordinate their activities, such as nutrient
69 acquisition, metabolism, and defence mechanisms¹¹. The protective EPS barrier, reduced
70 growth rates, high density of the bacterial cells, and the prevalence of persister cells within the
71 biofilm enhance resistance to antibiotics, disinfectants, host immune defences, desiccation, and
72 nutrient limitations, compared to planktonic bacteria. Eventually, environmental cues trigger
73 the dispersion of cells from the biofilm, allowing them to colonise new surfaces and repeat the
74 cycle. This entire process and the protective environment that the biofilm provides¹²⁻¹⁴
75 contributes to the persistence and chronicity of biofilm-associated infections¹⁵⁻¹⁸, which are
76 challenging to treat and eradicate¹⁹⁻²⁴.

77 In healthcare settings, opportunistic pathogens frequently contribute to healthcare-associated
78 infections (HAIs)^{25,26}. HAIs are infections that patients acquire while receiving treatment for
79 medical or surgical conditions within a healthcare setting, such as hospitals, outpatient clinics,
80 nursing homes, and long-term care facilities. HAIs significantly increase medical care costs,
81 length of hospital stays, and mortality rates. It is predicted that nearly 3.5 million people could



82 lose their lives due to HAIs every year, up to 2050²⁷. Approximately 80% of HAIs can be
 83 attributed to biofilms, therefore, representing one of the greatest challenges in healthcare^{7,24,28}.



84

85 **Figure 1. A schematic of bacterial adhesion and biofilm formation on a surface.** Free-
 86 floating bacteria land on the surface, produce EPS, and become part of a resilient bacterial
 87 biofilm. Eventually, bacteria will disperse, resulting in the colonisation of new environments.
 88 Created using BioRender.

89

90 1.2. Chemical approaches for managing bacteria and biofilms

91 Antibiotics are medications that are used to treat or prevent some types of bacterial infection.
 92 The extensive use of antibiotics is due to their broad range of effects, which include blocking
 93 the formation of bacterial cell walls, damaging cell membrane integrity, interfering with the
 94 production of nucleic acids and proteins, and disrupting essential metabolic processes.
 95 Therefore, it represents a first-choice drug for patients with an infection^{29–31}. However, due to
 96 the protective nature of biofilms, these infections are often resistant to conventional
 97 antibiotics¹⁴. Therefore, the misuse and overuse of antibiotics have encouraged the
 98 development of antibiotic-resistant bacteria, further contributing to the development of chronic,
 99 life-threatening infections^{32,33}.

100 Alongside antibiotics, disinfectants and chemical sanitisers are widely used to manage bacteria
 101 within healthcare settings to reduce HAI incidence. However, repeated use is practically and
 102 economically challenging. Moreover, there is growing evidence that extended interaction with
 103 such chemicals for sanitisation purposes (chlorine, hydrogen peroxide, sodium hypochlorite,
 104 ethanol) can lead to the enhanced probability of contracting long-term heart and lung
 105 diseases^{34–37}.



106 Another chemical-based approach worthy of attention within healthcare settings is the
107 application of metal-based surface coatings^{38,39}. These coatings incorporate metal ions (e.g.,
108 silver, copper, zinc), metal oxides, or metal-organic frameworks^{40–42}, offering broad-spectrum
109 antimicrobial activity through mechanisms such as reactive oxygen species (ROS) generation
110 and bacterial membrane disruption^{26,43–46}. Despite their demonstrated antibacterial potential,
111 several challenges hinder their widespread application. Ensuring stability under real-world
112 conditions remains difficult, and the protective EPS matrix of biofilms can restrict ROS
113 penetration. For example, silver-coated catheters are currently on the market with the ability to
114 prevent infection for several days, but ultimately, result in biofilm formation, restricting long-
115 term use^{47,48}. Moreover, coating efficacy is highly dependent on factors such as application
116 method, environmental conditions, and surface cleanliness⁴⁹. The non-selective toxicity of
117 metals and potential for metal ion leaching can lead to cytotoxicity and adverse host effects,
118 posing significant barriers to clinical translation^{50,51}.

119 Due to the nature of antibiotics, disinfectants, and metal-based coatings putting selective
120 pressure on microbes, they result in increased risk of antimicrobial resistance (AMR)
121 development^{39,52–55}. AMR poses a severe and escalating global health threat, pushing 24
122 million more people into extreme poverty in the next decade, and by 2050, will result in 10
123 million deaths annually and have an economic impact of \$100 trillion^{56–58}. The spread of AMR
124 endangers essential medical procedures, such as surgeries and chemotherapy, which rely on
125 effective infection control; therefore, the development of new biofilm-prevention methods and
126 rigorous stewardship of existing antimicrobials are crucial.

127 Given this tremendous concern, there is an increasing motivation for designing and developing
128 antimicrobial surfaces that provide a sustainable approach to prevent biofilm formation and the
129 spread of infections, while reducing our reliance on antibiotics and harsh chemical agents.
130 Several reviews explore chemical-based approaches in more depth^{59–62}. This review focuses
131 primarily on physical approaches to managing bacteria and biofilms.

132

133 **2. Physical approaches for managing bacteria and biofilms**

134 *2.1. Background*

135 Using surface topography is an innovative approach to achieving antibacterial effects without
136 relying on chemical agents. By designing surfaces with specific patterns, such as ridges, spikes,
137 or pillars, bacteria are prevented from adhering, colonising, and forming a stable connection to



138 the surface to form a biofilm. Antibacterial surfaces can be broadly classified as either
139 antibiofouling, which repels or resists bacterial attachment, or bactericidal, which actively kills
140 bacteria. In some instances, an antibacterial surface may exhibit both antibiofouling and
141 bactericidal characteristics^{59,63–68}. This strategy offers an alternative approach to traditional
142 chemical-based methods to manage bacterial load. Such engineered topographies can be
143 applied to medical devices, implants, and high-contact surfaces to maintain sterility and
144 minimise infection risks within healthcare settings.

145

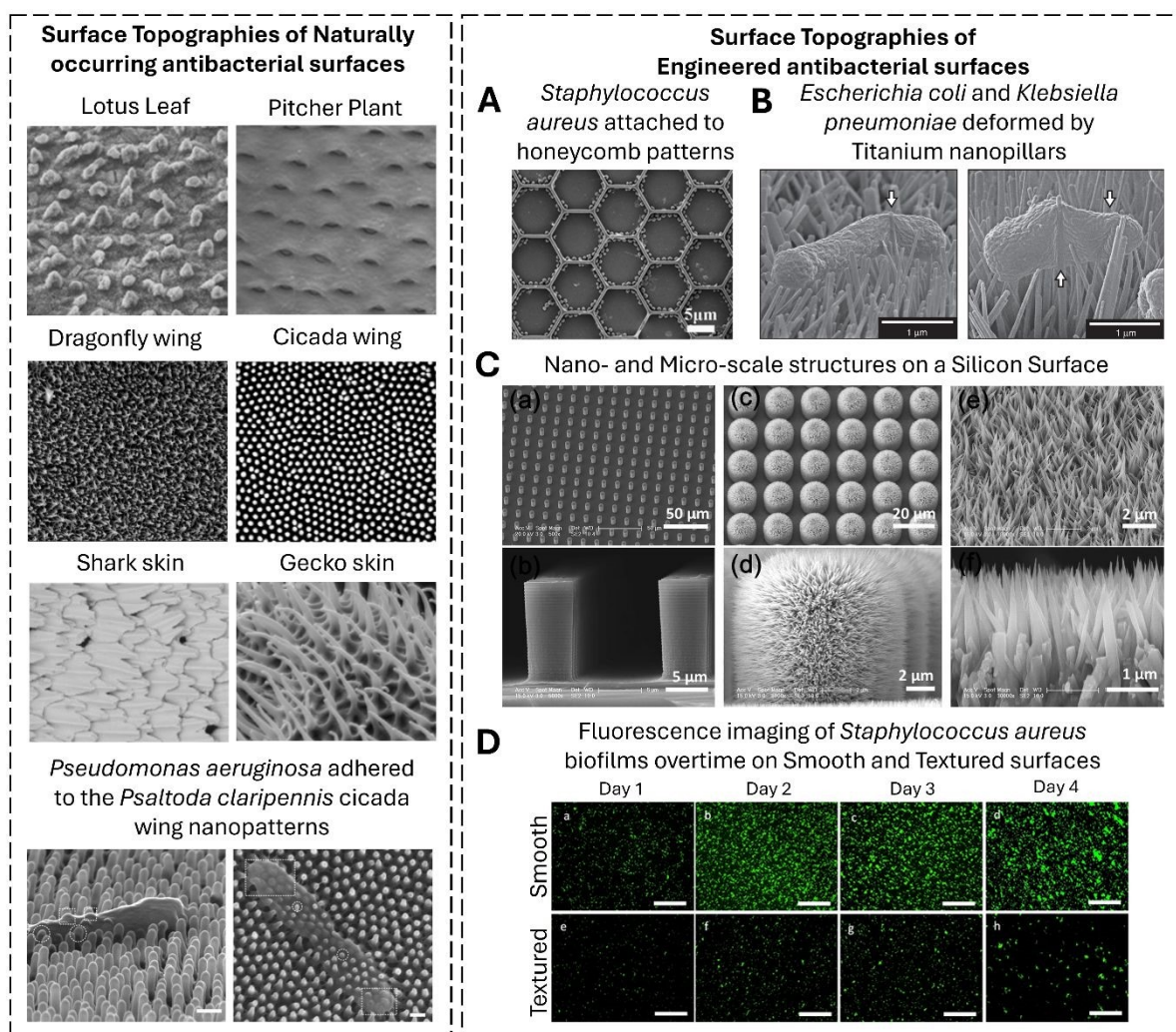
146 2.2. Nature-Inspired Biomimetic Antibacterial Physical Strategies

147 Nature is an unexhausted source of inspiration for scientists and engineers, particularly for the
148 development of biomimetic antibacterial and antifouling designs. Some natural surfaces have
149 developed the ability to resist or prevent bacterial colonisation and biofilm formation⁶⁹. These
150 surfaces include certain plant leaves, gecko feet, shark skin, insect wings, fish scales, and spider
151 silk, which are frequently studied for their self-cleaning, low-adhesive, and superhydrophobic
152 properties, many of which also confer antibacterial capabilities^{70,71}.

153 Several natural surfaces prevent microbial attachment through purely physical means, as shown
154 in **Table 1**. For instance, cicada wings feature high-aspect-ratio nanopillar arrays that
155 mechanically rupture bacterial membranes upon contact. As shown in **Figure 2**, *P. aeruginosa*
156 loses shape and turgor due to penetration from the wing features⁷². Unlike chemical coatings,
157 these surfaces rely on mechanical interactions to exert their bactericidal effects. Similarly,
158 shark skin is composed of dermal denticles, which create a rough surface topography that
159 reduces hydrodynamic drag and, therefore, microbial adhesion. The structured patterns alter
160 local fluid dynamics and create a level of turbulence, potentially minimising the time
161 microorganisms remain in contact with the surface and facilitating their removal^{73,74}. These
162 principles have been commercially translated, most notably being Sharklet[®], which replicates
163 key features of shark skin topography to reduce bacterial attachment. Sharklet[®] is a synthetic
164 surface fabricated via photolithography that mimics the ordered microtopography of dermal
165 denticles using interlocking diamond-shaped riblets. The efficacy of Sharklet[®] surface patterns
166 has been reviewed in more depth and demonstrates the varying efficacy depending on the
167 microbial species (47-99% reductions)^{63,75–78}, underscoring the inherent complexity of
168 biological systems and the different ways different bacterial species will respond to the same
169 surface.



170

View Article Online
DOI: 10.1039/D6LF00022C

171

172 **Figure 2. Naturally Occurring and Engineered Surface Topographies that demonstrate**

173 **antibacterial behaviour.** (Left) SEM images of naturally occurring surface features found on

174 the lotus leaf¹¹⁰, pitcher plant¹¹¹, dragonfly wing¹¹², cicada wing¹¹³, shark skin⁷³, and gecko

175 skin¹¹⁴, including *P. aeruginosa* losing shape and turgor on cicada wing patterns, with outlines

176 highlighting penetration and perturbation. Scale bars = 200nm⁷². (Right) SEM images of

177 engineered surface features to demonstrate antibacterial behaviour. (A) 5 μm honeycomb-like

178 patterns result in the random distribution and adhesion of *S. aureus* to the side walls¹¹⁵. (B) *S.*

179 *aureus* and *P. aeruginosa* (false coloured red) attached and ruptured by gold nanopillars¹¹⁶. (C)

180 Micro- and Nano-scale structures patterned on a silicon surface¹¹⁰. (D) Fluorescence images of

181 *S. aureus* biofilms being reduced on textured surfaces in comparison to smooth surfaces and

182 on textured surfaces overtime. Scale bar = 100 μm ¹¹⁷. Images were reprinted (adapted) with

183 permission. ¹¹⁰Jiang *et al.* (2020). Copyright 2020, Elsevier. ¹¹¹Moran *et al.* (2010), licensed under CC.

184 ¹¹²Kamarajan *et al.* (2020), licensed under CC. ¹¹³Pogodin *et al.* (2013). Copyright 2013, Biophysical

185 Society. ⁷³Chien *et al.* (2020). Copyright 2020, Elsevier. ¹¹⁴Watson *et al.* (2015). Copyright 2015,

186 Elsevier. ⁷²Velic *et al.* (2021). Copyright 2021, Elsevier. ¹¹⁵Yang *et al.* (2015). Copyright 2015,

187 Elsevier. ¹¹⁶Elbourne *et al.* (2019), licensed under CC. ¹¹⁷Khurshheed *et al.* (2024), licensed under CC.

188



189 It is important to note that the experimental methods to understand bacterial behaviour vary
190 reflecting a lack of standardisation and methodological uniformity across studies⁷⁹, as shown
191 in **Tables 2** and **3**. Commonly used methods to assess the antibacterial activity of surfaces
192 include viability staining with fluorescent dyes such as SYTO 9 and propidium iodide (PI),
193 colony-forming unit (CFU) counts, and imaging techniques such as confocal laser scanning
194 microscopy (CLSM), fluorescence microscopy, and scanning electron microscopy (SEM).
195 These approaches can provide complementary information, but each technique has notable
196 limitations. CFU counts enable quantification of viable, culturable bacteria; however, this
197 method often underestimates bacterial survival due to the presence of viable but non-culturable
198 (VBNC) populations or incomplete detachment of biofilms from surfaces^{80–83}.

199 Fluorescence-based assays and microscopy allow visualisation of cell viability and spatial
200 distribution. CLSM in particular can provide three-dimensional information on biofilm
201 structure, whereas SEM offers high-resolution imaging of bacterial morphology and surface
202 interactions^{84–86}. Fluorescent staining approaches can be influenced by staining conditions such
203 as dye concentration, incubation time, and biofilm thickness, which may affect dye penetration
204 and lead to misinterpretation of viability^{87–90}. Microscopy-based techniques rely on image
205 processing or fluorescence intensity measurements that can vary depending on imaging
206 parameters. In addition, SEM requires extensive sample preparation, which may alter biofilm
207 structure⁹¹. A further challenge across these methods is the lack of standardised protocols for
208 dye concentrations, incubation conditions, and quantification approaches, making comparisons
209 between studies difficult. Consequently, while these techniques are widely used to evaluate
210 antibacterial surfaces, careful methodological control and the combination of multiple
211 complementary assays are often necessary to obtain reliable and reproducible assessments of
212 antibacterial performance.

213 Biomimetic replication of features seen in nature has led to promising engineered surfaces. For
214 example, Kumar and Bhardwaj (2020) replicated the hierarchical structure of the taro leaf using
215 photolithography, achieving static contact angles up to 148° by mimicking the dual-scale
216 hexagonal and flake-like microstructures⁹². However, traditional fabrication methods, such as
217 photolithography, make the whole process costly and time-consuming, with limited scalability.
218 Therefore, there has been a lack of commercialisation of such surfaces. However, the research
219 and these examples underscore the effectiveness of biologically inspired surface topographies
220 in resisting bacterial colonisation and biofilm development.



221 For antibacterial surface topographies to achieve translational and commercial impact, scalable
222 and high-throughput manufacturing techniques need to be considered and used to produce
223 nano- and micro-scale features reliably and reproducibly over large areas, with relevant
224 materials, and on clinically relevant substrates. Roll-to-roll nanoimprint lithography offers
225 significant promise, enabling continuous pattern transfer onto polymer films at industrial
226 speeds with high reliability and relatively low cost per unit. In combination with nanocoating,
227 the manufacturing can also overcome the high cost associated with a master mould. This
228 approach is particularly attractive for disposable medical products, wound dressings, and
229 device surfaces, where large-area replication and throughput are critical^{93–95}. Roll-to-roll
230 nanoimprint lithography offers significant promise, enabling continuous pattern transfer onto
231 polymer films at industrial speeds with high reliability and relatively low cost per unit. In
232 combination with nanocoating, the manufacturing can also overcome the high cost associated
233 with a master mould. This approach is particularly attractive for disposable medical products,
234 wound dressings, and device surfaces, where large-area replication and throughput are
235 critical^{93–95}. Similarly, laser-based methods, such as laser-induced periodic surface structures
236 (LIPSS), provide a single-step method for creating features directly onto metallic or polymeric
237 surfaces. LIPSS is especially relevant for orthopaedic implants, surgical tools, and catheter
238 components, as it can be applied to complex geometries and hard materials while allowing
239 spatial control of patterning^{96–99}. Other scalable approaches, including injection moulding with
240 textured moulds^{100,101}, hot embossing^{102,103}, and reactive ion etching^{104,105}, also present
241 industrially viable routes, particularly when integrated into existing medical device
242 manufacturing pipelines.

243 However, for these techniques to be clinically feasible, they must demonstrate not only pattern
244 uniformity and reliability, but also compatibility with regulatory requirements, sterilisation
245 processes, mechanical durability, and cost constraints. Moreover, reproducibility across large
246 production batches and the ability to pattern three-dimensional, curved, or flexible substrates
247 remain practical challenges. A deeper consideration of manufacturing scalability, including
248 tooling lifetime, cycle time, material compatibility, and quality control metrology, will
249 therefore be essential to bridge the gap between laboratory proof of concept research and
250 commercially available antibacterial medical devices and healthcare equipment. Detailed
251 reviews of fabrication strategies and manufacturing techniques are available^{106,107}.

252 As mentioned, for physical antibacterial topographies to achieve translational feasibility, they
253 must demonstrate durable antimicrobial efficacy alongside mechanical and chemical stability



254 under real-world conditions. In clinical and industrial settings, the topographies would be
255 routinely exposed to extensive cleaning procedures, repeated sterilisation cycles, and frictional
256 wear. Francone *et al.* (2021) fabricated patterned polypropylene and conducted washability
257 tests mimicking hospital-specific cleaning protocols, which demonstrated that the features of
258 the surface, such as topography, water contact angle, and gloss, remained unchanged despite
259 intensive physical and chemical cleaning procedures over time¹⁰⁸. This demonstrates promise
260 for the application of nano- and micro-patterning within clinical settings. Theoretically, if the
261 patterns are not damaged, the surface can be reused indefinitely when cleaned¹⁰⁹. However,
262 from this literature review, it is seen that many studies show high initial promise but rarely test
263 the durability of the features against wear, fouling, and bacterial resistance, with more research
264 needing to be conducted within this area. Therefore, the rational design of antibacterial surface
265 topographies must integrate considerations of mechanical durability, chemical resistance, and
266 wear stability alongside antimicrobial performance to ensure function throughout the intended
267 lifespan of the surface.

View Article Online
DOI: 10.1039/D6LF00022C



268 **Table 1. Examples of Naturally Occurring Antibacterial Physical Surfaces**

Surface	Features	Fabrication Technique	Antibacterial Activity	Ref
Lotus Leaf (<i>Nelumbo nucifera</i>)	Micro-Papillae, 100 μm height and 100 μm spacing. Wax crystalloids, 1–5 μm in height. Tabular and convex papillae, 30–50 μm length and 10–30 μm width. Superhydrophobic (WCA = 162°)	Natural	Antibiofouling	118–120
Taro Leaf (<i>Colocasia esculenta</i>)	Nano (< 0.5 μm), micro (> 0.5 μm – 10 μm) and macro topographies (> 10 μm). Superhydrophobic (WCA = 164°)	Natural	Antibiofouling	118,121,122
Shark skin (<i>Carcharodon carcharias</i>)	Dermal denticles, 26.8 μm height, 99.5 μm spacing	Natural	Antibiofouling	123
Shark skin (<i>Centrophorus granulosus</i>)	Dermal denticles, 15.8 μm height, 136.8 μm spacing	Natural	Antibiofouling	123
Cicadas	<i>Megapomponia intermedia</i> , Pillars, 241 nm height, 156 nm diameter, 165 nm spacing <i>Ayuthia spectabile</i> , Pillars, 182 nm height, 207 nm diameter, 251 nm spacing <i>Cryptotympana Aguila</i> , Pillars, 182 nm height, 159 nm diameter, 187 nm spacing	Natural	Bactericidal against gram negative bacteria (<i>Pseudomonas fluorescens</i>)	124
Cicada Wing (<i>Psaltoda claripennis</i>)	Nanoneedles, 200 nm height, 170nm spacing. Superhydrophobic (WCA = 158 – 159°)	Natural	Bactericidal against gram negative bacteria (<i>Pseudomonas aeruginosa</i>)	67,125





Gecko (<i>Lucasium sp.</i>)	Skin	Spinule structures, 3000 nm height, 500 nm spacing, tip radius of curvature < 20 nm. Superhydrophobic (WCA = 150 – 155°)	Natural	Bactericidal against gram negative bacteria (<i>Porphyromonas gingivalis</i>)	¹¹⁴
Dragonfly (<i>Diplacodes bipunctata</i>)	wing	Nanopillars, 240 nm height, 200 nm spacing. Superhydrophobic (WCA = 153°)	Natural	Bactericidal against gram positive (<i>Bacillus subtilis</i>) and gram negative (<i>Pseudomonas aeruginosa</i>) bacteria	^{126–128}

270 2.3. Bactericidal Physical Surface Topographies

View Article Online
DOI: 10.1039/D6LF00022C

271 Bactericidal surface topographies are designed to actively kill bacteria through mechanical
272 forces. These surfaces often feature nanoscale structures such as spikes, pillars, or sharp ridges
273 that can promote adhesion and then stretch, puncture, or rupture bacterial cell membranes upon
274 contact, as they grow, or during movement, and if the applied force exceeds their elasticity,
275 leading to bacterial lysis and death. This deformation-stretching-torn apart effect has been
276 observed in various engineered surfaces, including biomimetic designs inspired by cicada and
277 damselfly wings^{113,129,130}. The ability of a bacterium to rupture due to a nanopatterned surface
278 may also depend on the maturation stage of the cell, as shown by Truong *et al.* (2017). The
279 nanopillars present on the wings of the damselfly (*Calopteryx haemorrhoidalis*) exhibited the
280 highest bactericidal activity in the early (1 hour) and late (24 hour) stationary phase of
281 *Staphylococcus aureus* and *Pseudomonas aeruginosa*, resulting in 89.7 and 61.3% as 97.9 and
282 97.1% dead cells upon surface contact, respectively¹³¹. These findings highlight that strong
283 bacterial adherence to the nanopatterned surface is critical for effective mechano-bactericidal
284 activity. High-aspect-ratio structures are particularly important for promoting initial bacterial
285 attachment, which facilitates subsequent membrane rupture, for example, hierarchical
286 structures like two-tiered micropillar arrays¹²⁹. The bactericidal performance of such surfaces
287 is strongly influenced by structural characteristics, including pillar height, diameter, density,
288 and spatial arrangement. Denser and smaller nanopillar arrays have been found to be more
289 effective against both Gram-negative and Gram-positive bacteria compared to larger, widely
290 spaced configurations¹³², because they need to promote adhesion to be able to demonstrate their
291 killing effect.

292 Other characteristics of bacteria, such as their motility, morphology, and size, can influence
293 their interactions with nanopatterned surfaces. Highly motile bacteria experience greater
294 membrane deformation due to movement across the surface, leading to increased cell
295 rupture¹³³. Morphological differences, such as being coccoid or rod-shaped, can impact their
296 interactions with the same surface. The relative dimensions of bacterial cells and surface
297 patterns are also critical. Bactericidal efficiency is enhanced when cell size exceeds the spacing
298 between nanopatterns, allowing for direct penetration and rupture. Conversely, smaller
299 bacterial cells may stretch or compress against the sidewalls of nanostructures, resulting in
300 different mechanical stress responses. Kelleher *et al.* (2016) demonstrated that surfaces with
301 tighter nanopillar spacing and smaller feature sizes showed superior bactericidal activity
302 compared to those with lower density and larger features¹²⁴. Modaresifar *et al.* (2019)



303 systematically reviewed bactericidal nanopatterning and reported that most design parameters
304 tend to fall within specific ranges: feature height between 100 – 1000 nm, diameter between
305 10 – 300 nm, and spacing less than 500 nm¹³⁴. A variety of materials and surfaces have been
306 explored to demonstrate bactericidal activity, for example, black silicon is widely used, which
307 is regular silicon etched to produce nanoscale markings that make it appear black due to
308 trapping of light¹³⁵. In order to show the breadth of research in this area, **Table 2** is generated
309 to summary the materials used, feature dimensions, fabrication techniques, bactericidal
310 activity, and how it is evaluated. It explores several examples of bactericidal surface patterns
311 with their respective features and what they are effective against.

312 A challenge in the field of antibacterial surface topographies is the lack of standardisation and
313 methodological uniformity across existing studies, which significantly limits comparison,
314 meta-analysis, and reproducibility. A critical evaluation by Redfern *et al.* (2024) revealed
315 substantial variation in growth conditions, controls, and analytical measurements of biofilms
316 performed by different research groups⁷⁹. Standardisation of microbiological practice is
317 inherently difficult due to differences in equipment, technical expertise, and laboratory
318 resources across institutions. Furthermore, biofilm science itself remains an evolving field,
319 with ongoing debate regarding the most appropriate methods to grow, control, quantify, and
320 analyse bacteria and biofilms.

321 In addition, there is often an inadequate characterisation of the topography. For example,
322 relying on parameters like average roughness, which does not describe the dimensions of the
323 pattern itself¹³⁶. Surfaces with identical roughness values may have different heights, widths,
324 spacing, and shapes, which also significantly impact how bacteria interact with the surface.
325 Researchers must provide sufficient details of topographical descriptors such as feature height,
326 width, spacing, shape, surface chemistry, etc., as well as experimental conditions such as
327 bacterial strain selection, growth phase, inoculum density, media composition, incubation
328 duration, and environmental parameters, in addition to reasoning behind quantitative outcome
329 measures.

330 Interactions at the bacteria-surface interface are complex, dynamic, and heavily dependent on
331 specific environmental conditions. There is no ‘one-size-fits-all’ solution with patterned
332 surfaces, and the features need to be tailored depending on the bacterial species and the
333 environment it will be experiencing. The optimisation of pattern design, including parameters



334 such as feature density, stiffness, and geometry, is therefore needed to enhance the antibacterial
335 surface performance for different bacterial species^{137–139}.

336 Optimal topographical design is likely to be context specific. A micro- or nano-scale pattern
337 that reduces bacterial colonisation on a dry, high-touch hospital surface may not perform
338 equivalently on an implanted medical device, where continuous fluid flow, immune
339 interactions, and long-term mechanical stresses alter bacterial behaviour. Therefore, proposed
340 best practices should not only encourage comprehensive reporting of surface parameters,
341 microbiological conditions, and quantitative antibacterial measurements, but also require clear
342 justification of experimental models in relation to the intended end-use environment.
343 Establishing such a structured reporting framework would enhance reproducibility, enable
344 meaningful comparisons, and provide a more rigorous foundation for translating antibacterial
345 topographic surfaces into clinically and industrially relevant applications.

346

347

348

349

350

351

352

353

354

View Article Online
DOI: 10.1039/D6LF00022C



355 **Table 2. Examples of Bactericidal Physical Surface Topographies.** *Material chemistry may synergise with surface structures to demonstrate
 356 antibacterial effect. Propidium Iodide (PI). Colony forming unit (CFU). Confocal laser scanning microscopy (CLSM). Scanning Electron Microscopy (SEM).
 357 Atomic force microscopy (AFM).

Surface	Features	Fabrication Technique	Antibacterial Activity Testing Methods	Bactericidal Efficacy	Ref
Black Silicon	Nanograss, 500 nm height, 20 – 80 nm diameter. Hydrophilic (WCA = 80°)	Reactive Ion Etching	SYTO 9/PI CLSM CFU counts	Effective against gram positive (<i>Bacillus subtilis</i>) and gram negative (<i>Pseudomonas aeruginosa</i>) bacteria	¹²⁶
Black Silicon	Nanograss, 4 µm height, 220 nm diameter. Superhydrophobic (WCA = 154°).	Deep Reactive Ion Etching	SYTO 9/PI Fluorescence microscopy CFU counts	Effective against gram positive (<i>Staphylococcus aureus</i>) and gram negative (<i>Escherichia coli</i>) bacteria	¹⁴⁰
Black Silicon	Nanopillars 280 nm height, Superhydrophilic (WCA = 8.4° ± 2.1°). 430 nm height, Hydrophilic (WCA = 12.4° ± 1.2°). 610 nm height, Superhydrophilic (WCA = 9.9° ± 1.0°)	Plasma etching	SYTO 9/PI CLSM SEM	Effective against gram positive (<i>Staphylococcus aureus</i>) and gram negative (<i>Pseudomonas aeruginosa</i>) bacteria	¹⁴¹

Diamond-coated* Black Silicon	Nanoneedles, 0.5–1 μm height (short needle) and 15–20 μm height (long needle)	Plasma etching and vapour deposition	SYTO 9/PI Fluorescence microscopy SEM	Effective against gram negative (<i>Pseudomonas aeruginosa</i>) bacteria	¹⁴²
Cicada-inspired Diamond* surface	Nanocones with sharp tips, 3–5 μm height, 10–40 nm tip diameter, 350 nm–1.2 μm nanocone width	Microwave plasma chemical vapour deposition and reactive ion etching	SYTO 9/PI Fluorescence microscopy SEM	Effective against gram negative (<i>Pseudomonas aeruginosa</i>) bacteria	¹⁴³
Dragonfly-inspired Titanium (Ti)* nanopatterned array	Nanowires, average diameter 40.3 nm. Hydrophilic (WCA = 73°).	Hydrothermal etching	SYTO 9/PI CLSM SEM	Effective against gram negative (<i>Pseudomonas aeruginosa</i>) bacteria	¹⁴⁴
Cicada wing-inspired Ti* columns	Nanocolumns, 478 \pm 6 nm height. Nano-sized grains, 33 \pm 7 nm width. 26 \pm 3 nm (R_q) surface roughness. Hydrophilic (WCA = 41.48° \pm 0.83°)	Glancing angle sputter deposition	SYTO 9/PI Fluorescence microscopy SEM	Effective against gram negative (<i>Escherichia coli</i>) bacteria	¹⁴⁵
Ti alloy* surface	Nanospikes, 2 μm height, 10 nm diameter, 2 μm spacing	Anodisation	SYTO 9/PI Fluorescence microscopy SEM	Effective against gram positive (<i>Staphylococcus aureus</i>) bacteria	¹⁴⁶
Ti alloy* surface	Nanospikes, 20 nm diameter	Thermal oxidation	SYTO 9/PI Fluorescence microscopy PrestoBlue®	Effective against gram negative (<i>Escherichia coli</i>) bacteria	¹⁴⁷





Cicada-inspired Titania* nanowire arrays	Nanowires Brush type: 100 nm diameter Niche type: 10–15 μm diameter	Hydrothermal process	SYTO 9/PI Fluorescence microscopy PrestoBlue® SEM	Effective against motile bacteria (<i>Pseudomonas aeruginosa</i> , <i>Escherichia coli</i> and <i>Bacillus subtilis</i>)	¹⁴⁸
Titania* Micro-nanopillar arrays	Pillar array sizing 20 μm , 10 μm , 5 μm , 2 μm , 1.4 μm , 1.2 μm , 1.0 μm , 0.8 μm , and 0.6 μm Hydrophilic (WCA < 90°)	Photolithography, RF magnetron sputtering and thermal oxidation	SYTO 9/PI CLSM SEM	Effective against gram positive (<i>Staphylococcus aureus</i>) and gram negative (<i>Escherichia coli</i>) bacteria	¹⁴⁹
Aluminium (Al 6063 alloy) nanostructured surface	Etching time: 0.5 hr, 69.9 \pm 5.3 nm (R_{rms}), Hydrophilic (WCA = 28.2° \pm 3.3°). 1 hr, 133.6 \pm 36.1 nm (R_{rms}), Hydrophilic (WCA = 21.8° \pm 4.7°). 3 hr, 995 \pm 114.7 nm (R_{rms}), Hydrophilic (WCA = 17.7° \pm 4.3°)	Wet chemical etching	SYTO 9/PI Fluorescence microscopy	Effective against gram positive (<i>Staphylococcus aureus</i>) and gram negative (<i>Pseudomonas aeruginosa</i>) bacteria	¹⁵⁰
Cicada wing-inspired PMMA nanopatterned surface	Nanopillars, 200 – 300 nm height, 70–215 nm diameter, 130 – 380 nm spacing	Nanoimprint lithography	SYTO 9/PI Fluorescence microscopy CFU counts SEM AFM	Effective against gram negative (<i>Escherichia coli</i>) bacteria	¹⁵¹

Poly-L-lactic acid (PLLA) surface	Cylindrical micropillars, 40 μm height, 40 μm width decorated with nanostructures. Hydrophobic (WCA $>100^\circ$).	Nanoimprint lithography	ISO 207043:2007 CFU counts SEM	Effective against gram positive (<i>Staphylococcus aureus</i>) and gram negative (<i>Escherichia coli</i>) bacteria	¹⁵²
Polycarbonate surface	Nanopillars arrays, 143 – 408 nm height, 100 – 313.9 nm spacing. Hydrophobic.	Nanoporous anodic aluminium oxide (AAO) template-assisted hot embossing and wet etching	SYTO 9/PI Fluorescence microscopy SEM	Effective against gram negative (<i>Escherichia coli</i>) bacteria	¹⁵³
Gecko skin-inspired nano-spinules	Spinules, 1 – 4 μm height, 600 nm spacing. Hydrophobic (WCA = 134°).	Nano-templating	SYTO 9/ TO-PRO-3 Laser confocal microscopy SEM	Effective against gram positive bacteria (<i>Lactobacillus</i>)	¹⁵⁴
Cicada wing-inspired Gold (Au)* nanopatterns	Nanopillars (100 nm height, 50 nm diameter) Nanorings (100 nm height, 100–200 nm diameter) Nanonuggets (100 nm height, 100–200 nm diameter)	Electrodeposition and plasma etching	SYTO 9/PI Fluorescence microscopy SEM	Effective against gram positive (<i>Staphylococcus aureus</i>) bacteria	¹⁵⁵
PDMS or PMMA nanopatterns	Moth-Eye Nanocones, 250 nm diameter at the base and 80 nm on the top, 350 nm height and 250 nm spacing.	PDMS – Soft lithography PMMA – Thermal nanoimprint lithography	SYTO 9/PI Fluorescence microscopy SEM	Effective against gram positive (<i>Staphylococcus aureus</i>) and gram negative (<i>Escherichia coli</i>) bacteria	¹⁵⁶



359 2.4. Antibiofouling Physical Surface Topographies

360 Antifouling surface topographies are engineered to prevent bacterial adhesion and colonisation
361 rather than directly killing the cells. The surface features often create an energetically
362 unfavourable environment for microbial attachment, or geometries that physically limit the
363 ability of bacteria to establish stable contact. Table 3 explores some examples of antibiofouling
364 surfaces along with the species they are reported to be successful against. As shown, these
365 features range from the nano- to the micro-scale; however, the broader literature provides a
366 fragmented, often incomplete, and potentially contradictory view of antifouling features and
367 what works best. For example, Kargar *et al.* (2014) reported that larger spherical features
368 delayed biofilm formation compared to smaller ones¹⁵⁷. Yet literature often recommends
369 smaller topographic sizes to inhibit biofilm formation^{158,159}.

370 Mok *et al.* (2019) showed that concave periodic boundary geometries limited *Escherichia coli*
371 accumulation¹⁶⁰, while Gu *et al.* (2017) demonstrated that hexagonally arranged topographies
372 with optimised spacing disrupt intercellular interactions and limit biofilm formation¹⁶¹. In
373 another study, Gu *et al.* (2016) further demonstrated that bacterial orientation tends to align
374 perpendicularly to linear patterns, with more random attachment occurring as line widths
375 increase and approach planar surfaces¹⁶². Ge *et al.* (2019) attributed antibacterial efficacy (e.g.,
376 62% reduction in *S. aureus* adhesion, and 73% reduction in *E. coli* adhesion) to the synergistic
377 effects of reduced contact area and spatial confinement offered by pillar-based topographies¹⁴⁹.
378 However, it is important to note that this group used Titanium oxide, which is inherently
379 antibacterial; therefore, potential effects may not solely be due to physical approaches. In
380 **Tables 2 and 3**, an annotation (*) has been made where groups have used materials that may
381 have particular chemistries that may synergise with surface structures to demonstrate an
382 antibacterial effect; the result is not entirely through physical means. It is important to note that
383 a major benefit of antibacterial activity through physical mechanisms induced by nano- and
384 micro-scale topographies is that they do not exert selective pressure for resistance development
385 like conventional antibiotics and other chemical-based methods do^{163,164}. However, long-term
386 efficacy and other potential impacts require further study^{164,165}.

387 Antifouling topographies reduce the likelihood of biofilm formation by making it difficult for
388 bacteria to remain anchored long enough to multiply and produce EPS, through the alteration
389 of surface properties such as roughness, contact forces, wettability, shear stress, and fluid flow.
390 Increased surface roughness reduces bacterial adhesion by limiting available adhesion points.



391 The reduction in contact area also impacts surface charge accumulation and distribution, therefore, altering the attractive and repulsive forces between the bacteria and the surface^{138,166,167}. Effectively, repelling the bacteria and reducing bacterial attachment.

394 Wettability also plays a crucial role in antibiofouling¹⁶⁸. Superhydrophobic surfaces (water contact angle $>150^\circ$) trap air pockets, creating a barrier against bacterial attachment, while superhydrophilic surfaces (water contact angle $<5^\circ$) form a continuous water layer that prevents direct contact with bacteria¹⁶⁹. Hierarchical structures, such as those found on lotus leaves, exhibit extreme wettability due to the combination of micro-scale bumps and nanoscale hairs. These structures allow water droplets to bead up and roll off easily, effectively preventing bacterial colonisation through self-cleaning mechanisms. A study developing titanium-based lotus leaf-like surfaces found that bacteria were unable to adhere due to trapped air nano- and micro-bubbles, which minimised contact and imparted antifouling properties¹⁷⁰. Ellinas *et al.* (2017) reported that a superhydrophobic polymethyl methacrylate (PMMA) surface with a water contact angle (WCA) above 155° exhibited prolonged bacterial repellence against *Synechococcus* sp. for up to 72 hours and minimised adhesion for four days¹⁷¹. However, superhydrophobicity typically diminishes during prolonged immersion in liquid due to air layer depletion. Therefore, careful control of feature size and surface design is essential to sustain the air layer and preserve antibacterial efficacy, and the design must be tailored to the specific environment in which it will be applied to achieve the greatest effect.

410 While a substantial body of literature explores surface topographies influencing bacterial attachment and biofilm formation, considerably fewer studies focus on elucidating the underlying mechanisms responsible for these effects. A deeper mechanistic understanding of how and why specific surface features inhibit biofilm development is therefore required. One mechanism of action might be the interruption of cellular signalling. As previously mentioned, quorum sensing is a form of bacterial cell-to-cell communication^{11,172}. Disrupting signalling capabilities may, in turn, disrupt stable, long-term contact of bacteria with a surface. Recent work with *P. aeruginosa* has explored the influence of nanotopographies on quorum-sensing molecule (QSM) production and their ability to reduce major virulence pathways¹⁷³. In addition, Romero *et al.* (2025) were able to explore that microtopographies resulted in quorum-sensing-mediated autolubrication that inhibits early-stage *P. aeruginosa* biofilm formation. It appears that the spatial restrictions of the topographies result in the production of lubricating rhamnolipids that prevent irreversible bacterial adhesion to the surface¹⁷⁴.



423

424 Other potential methods for topographies to induce antibacterial effects include altering surface
425 contact area, therefore reducing stable attachment and disrupting the spatial organisation
426 required for biofilm formation. It is also seen that topographies can influence hydrodynamic
427 forces in the near-surface environment, increasing velocity, which can disrupt initial bacterial
428 settlement. It is possible that the presence of patterns on the surface and their effect on the
429 surrounding environment would influence quorum sensing by limiting the effective diffusion
430 and local accumulation of autoinducers, preventing them from reaching the threshold
431 concentrations necessary to trigger coordinated gene expression required for stable attachment
432 and biofilm formation^{175–178}. Such mechanistic insights will enable a more comprehensive
433 interpretation of existing results, provide further validation of observed antimicrobial
434 performance, and support the rational design and broader application of topographically
435 engineered surfaces across diverse environments.

436 By optimising surface topography, including feature dimensions, spacing, and wettability
437 characteristics, antibiofouling surfaces can effectively minimise bacterial adhesion and biofilm
438 development, providing a promising strategy for antimicrobial surface design. Recently, the
439 use of machine learning (ML)¹⁷⁴ and artificial intelligence (AI)¹⁷⁹ to determine the best
440 antimicrobial shapes and features promises accelerated discovery. Yet these methods are
441 limited by the complexity of biological systems, which are difficult to emulate, and the lack of
442 standardised data on topographies and their performance, which can reduce the model's
443 accuracy. It is essential to consider the specific type of bacteria being targeted, as well as the
444 environmental conditions in which the surface will be applied, since these factors strongly
445 influence the effectiveness of the design. Because they focus on prevention and reduction rather
446 than destruction, antibiofouling topographies are especially valuable in applications where
447 long-term resistance to biofilm growth is needed, and they can be combined with chemical
448 coatings or bactericidal features to provide more comprehensive antibacterial protection.

449



450 **Table 3. Examples of Antifouling Physical Surface Topographies.** *Material chemistry may synergise with surface structures to demonstrate
 451 antibacterial effect. Propidium Iodide (PI). Confocal laser scanning microscopy (CLSM). Scanning Electron Microscopy (SEM). Colony forming
 452 unit (CFU). Green fluorescent protein (GFP).

Surface	Features	Fabrication Technique	Antibacterial Activity Testing Methods	Antifouling Efficacy	Ref
Silicon micropillar arrays	Various sizings: 20 μm , 10 μm , 5 μm , 2 μm , 1.4 μm , 1.2 μm , 1.0 μm , 0.8 μm , and 0.6 μm . Hydrophilic (WCA < 90°)	Photolithography and dry etching	SYTO 9/PI CLSM SEM	Effective against gram positive (<i>Staphylococcus aureus</i>) and gram negative (<i>Escherichia coli</i>) bacteria	¹⁸⁰
Silicon honeycomb pattern with micro-size pores	Pore sizes: 0.5 μm , Hydrophilic (WCA = 70° \pm 4°) 1 μm , Hydrophobic (WCA = 100° \pm 2°) 3 μm , Hydrophobic (WCA = 118° \pm 1°) 5 μm , Hydrophilic (WCA = 84° \pm 2°) 10 μm , Hydrophilic (WCA = 80° \pm 2°)	Photolithography and deep reactive ion etching	SYTO 9 CLSM SEM	Effective against gram positive (<i>Staphylococcus aureus</i>) and gram negative (<i>Escherichia coli</i>) bacteria	¹¹⁵
Lotus leaf-inspired Ti* surface	Micro-grains (10–20 μm), Nano-undulations (<200 nm).	Femtosecond laser irradiation	SYTO 17/ Concanavalin A Alex Fluor 488	Effective against gram positive (<i>Staphylococcus aureus</i>) and	¹⁸¹





	Superhydrophobic (WCA = 166°).		CLSM SEM	gram negative (<i>Pseudomonas aeruginosa</i>) bacteria	
Ti* mesopores	Pores, 20–25 nm diameter, ~17 nm (R_{rms}) surface roughness	Chemical oxidation	SEM	Effective against gram positive (<i>Staphylococcus aureus</i>) and gram negative (<i>Escherichia coli</i>) bacteria	182
Lotus leaf-inspired Ti alloy* surface	Various surface textures (390 nm, 660 nm, and 1.1 μ m)	Laser texturing	SEM	Effective against gram negative (<i>Escherichia coli</i>) bacteria	122
Nanostructured PMMA film	Nanopores, 460 nm depth, 300 nm spacing. Hydrophobic (WCA = 114.5°)	Nanoimprint lithography	GFP-expression Fluorescence microscopy	Effective against gram negative (<i>Pseudomonas aeruginosa</i> and <i>Escherichia coli</i>) bacteria	183
Shark skin-replicated PMMA microstructure	Tail abdomen denticles, 164.5 μ m height, 85.7 μ m width, 118.8 denticles/mm ² . Hydrophobic (WCA = 115.8°) Pectoral fin denticles, 166.2 μ m height, 69.8 μ m width, 83.3 denticles/mm ² . Hydrophobic (WCA = 105.6°)	Polymer imprinting	Crystal Violet	Effective against gram positive (<i>Staphylococcus aureus</i>) and gram negative (<i>Escherichia coli</i>) bacteria	73
PDMS micropatterned surface	Square features, 6 μ m height, 4 μ m spacing. Circular features, 3 μ m diameter, 2 μ m spacing. Ridges, 2 μ m	Soft lithography	Quantified manually SEM	Effective against gram positive (<i>Staphylococcus aureus</i> and <i>Staphylococcus epidermidis</i>) bacteria	184

	width and 3 μm -wide channels. Hydrophobic (WCA = 108.7°)				
Polystyrene spheres	630–1550 nm monodisperse spheres	Colloidal crystal fabrication	Light microscopy SEM	Effective against gram negative (<i>Pseudomonas aeruginosa</i>) bacteria	157
Polypropylene (PP) films	Micropillars, 10 μm height, 10 μm diameter, 23 μm spacing. Nanospikes, 2.2 μm height, 300nm base diameter. Hydrophobic (WCA >100°).	Nanoimprint lithography and reactive ion etching	Touch transfer assay CFU count	Effective against gram positive (<i>Staphylococcus aureus</i>) and gram negative (<i>Escherichia coli</i>) bacteria	108
Shark skin-mimicked chitosan*/graphene oxide* membranes	Topographies from the skin of a Basking Shark (<i>Cetorhinus maximus</i>)	Negative Mold	ISO 22196 CFU count MTT assay SEM	Effective against gram positive (<i>Staphylococcus aureus</i>) and gram negative (<i>Escherichia coli</i>) bacteria	185
Nanostructure sutures	Lamella structure, 500 nm length, 100 nm thickness	Plasma etching	SYTO 9/PI Fluorescence microscopy CFU counts SEM	Effective against gram negative (<i>Escherichia coli</i>) bacteria	186
Structured polystyrene surface	Lamella structures, 0.47 μm width, 2 μm spacing	Direct laser interference patterning	CFU counts SEM	Effective against gram positive (<i>Staphylococcus aureus</i>) bacteria	187

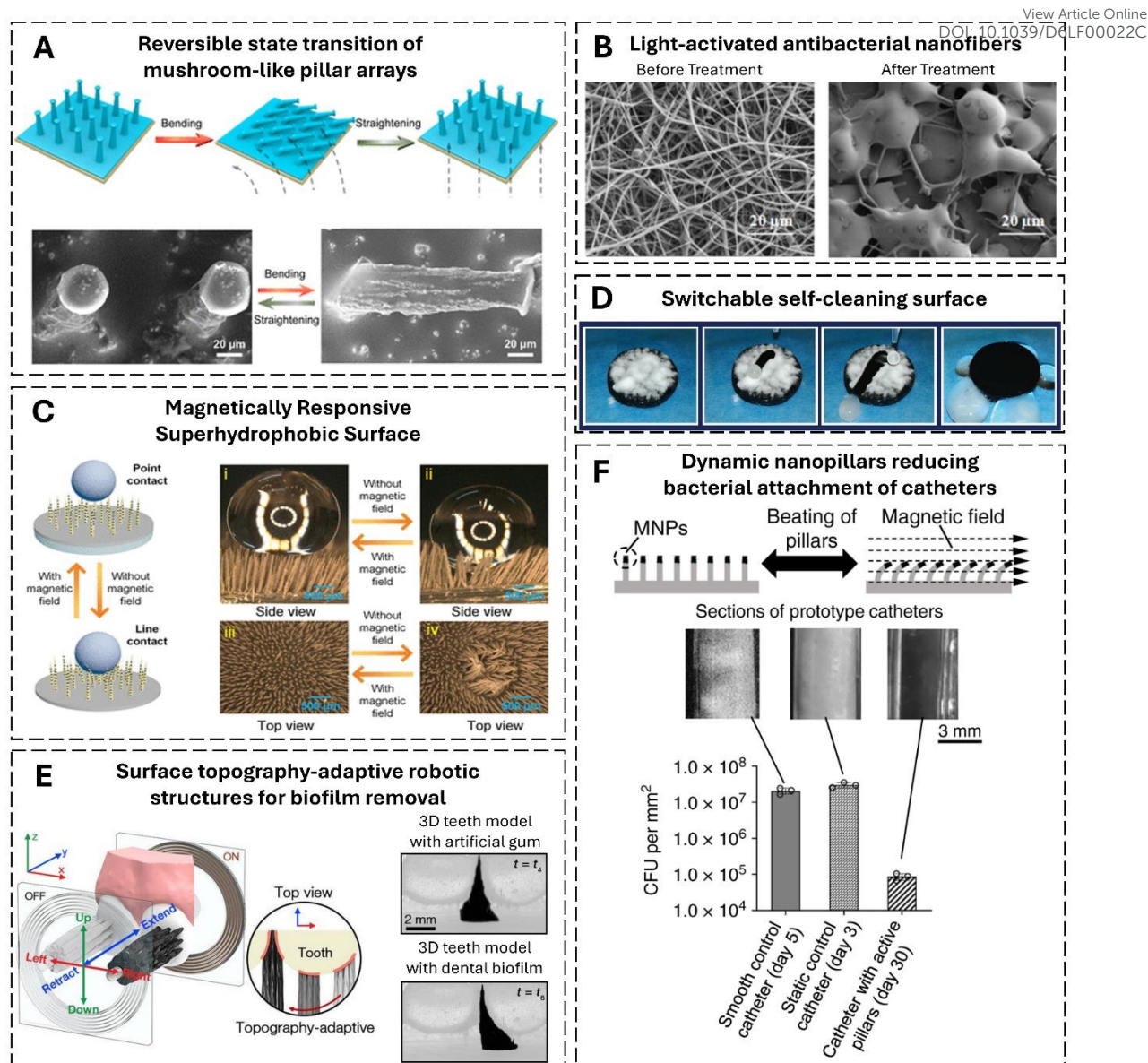


454 3. Next-Generation Dynamic Surface Topography

View Article Online
DOI: 10.1039/D6LF00022C

455 Dynamic or ‘smart’ physical surface technologies represent a new frontier in antibacterial
456 physical surface design. Unlike static topographies, these surfaces can adapt their physical
457 properties, such as shape, size, stiffness, or wettability, in response to external stimuli like
458 temperature, pH, light, or mechanical force (**Figure 3**). This adaptability allows them to
459 actively resist or disrupt microbial adhesion and biofilm formation in changing
460 environments^{188–190}. For instance, thermoresponsive coatings can switch between hydrophilic
461 and hydrophobic states, detaching adhered bacteria upon environmental changes. Similarly,
462 shape-memory or magnetically actuated surfaces can generate mechanical forces that
463 physically dislodge attached cells¹⁹¹. In addition, the development of surface topography-
464 adaptive robotic superstructures, capable of extending and retracting to dynamically adjust
465 their shape, length, and stiffness, offers a promising approach for effective and targeted biofilm
466 removal¹⁹². These dynamic systems offer a promising strategy for prolonging surface efficacy
467 and minimising microbial resistance development by introducing unpredictable and variable
468 adhesion conditions.





469
470 **Figure 3. Next-Generation Dynamic Surface Topography.** (A) Schematic and SEM images
471 of reversible bending and stretching of mushroom-like pillars allowing for the creation of a
472 superamphiphobic surface¹⁹³. (B) *meso*-tetraphenylporphyrin (TPP)/ polymethylmethacrylate
473 (PMMA) nanofibers before and after a 20-hour light-emitting diode treatment¹⁹⁴. (C)
474 Schematic and optical microscopy images showing magnetorheological elastomer micropillars
475 transformed from collapsed morphology (water-adhesive state) to the fully upright position
476 (water-repellent state)¹⁹⁵. (D) Self-cleaning surfaces showing flour powder contamination
477 preferentially adhering to water droplets and being successfully removed by fast drop
478 slipping¹⁹⁶. (E) The forward electromagnet core guides the robotic superstructure bristles
479 across the target surface, allowing for topographical adaptation, shape variation, and deep
480 penetration into interdental space for biofilm removal¹⁹². (F) Schematic of magnetic nanopillars
481 (MNPs) moving due to magnetic field. The representative images show the complete blockage
482 (visible white substance) of static control and flat control catheters, while the prototype
483 catheters with MNPs remained clear, resulting in lower CFU per mm^2 ¹⁹¹. Images were reprinted
484 (adapted) with permission. ¹⁹³Wang *et al.* (2019). Copyright 2019, American Chemical Society.
485 ¹⁹⁴Elashnikov *et al.* (2016). Copyright 2016, Elsevier. ¹⁹⁵Yang *et al.* 2018. Copyright 2018, American



486 Chemical Society. ¹⁹⁶Děkanovský et al. 2019. Copyright 2018, WILEY. ¹⁹²Jun Oh *et al.* (2024), licensed under CC. ¹⁹¹Gu et al. (2020), licensed under CC.

488

489 **4. The advantages and limitations of physical antibacterial approaches**

490 Using surface topography to reduce bacterial adhesion and biofilm formation within the
491 healthcare sector offers several significant advantages. Enhanced infection control is a primary
492 benefit, as physical antibacterial strategies can substantially lower the risk of HAIs by creating
493 surfaces inherently resistant to bacterial colonisation. This is especially crucial on medical
494 devices and in hospitals and clinics, where stringent infection control is essential^{160,108,197}.
495 Surface topographies could be strategically implemented on high-risk areas to passively reduce
496 bacterial attachment and biofilm formation, thereby lowering the risk of pathogen transmission
497 without reliance on reapplying chemical antimicrobial agents.

498 Physical surface strategies often exhibit broad-spectrum activity, being effective against a wide
499 range of bacterial species, including both Gram-positive and Gram-negative bacteria, which is
500 advantageous in diverse healthcare environments^{198,199}. Furthermore, because these strategies
501 do not depend on specific molecular targets, bacteria are less likely to develop resistance,
502 thereby mitigating the growing issue of AMR^{200–202}.

503 Environmentally, physical approaches are more sustainable and eco-friendlier, as they do not
504 involve the release or leaching of potentially harmful chemicals or metals over time^{108,203,204}.

505 This makes them particularly suitable for applications where biocompatibility is crucial, such
506 as in medical implants. With recent research supporting the use of topographies to control
507 bacterial colonisation while supporting mammalian cell attachment and tissue integration^{106,156}.

508 Lastly, the versatility of physical antibacterial techniques allows their application to a wide
509 range of materials and devices, including metals, polymers, and ceramics, allowing for tailoring
510 and engineering to suit specific applications and environments, and the creation of customised
511 antibacterial solutions¹⁹⁸.

512 Despite these advantages, there are also notable challenges in implementing these strategies.
513 Manufacturing process considerations need to be made to ensure the pattern chosen is scalable,
514 as techniques such as lithography, plasma treatments, or laser ablation might be intricate, time-
515 consuming, and costly, which may limit large-scale applications^{205,206}. Integrating these
516 technologies into existing healthcare infrastructure could be complex, necessitating substantial
517 modifications to current practices and equipment. In turn, this can result in a high initial cost



518 for implementation, due to the need for specialised equipment and processes, which can be a
519 barrier to widespread adoption, particularly in resource-limited settings.

520 Due to the success of patterning surfaces to demonstrate antibacterial effects *in vitro*, various
521 trials have explored their use *in vivo*. A review exploring nanopatterned titanium implants
522 showed that effectiveness varied between preclinical studies and the *ex vivo* and *in vivo*
523 experiments. Even though antibacterial activity was often seen in comparison to the control, it
524 was noted that the patterns were not sufficient to target chronic bone infections²⁰⁷. Patterning
525 of surfaces should not be seen as a replacement for antibiotics or cleaning methods, but as an
526 additional measure to provide bacterial colonisation and biofilm control. While physical
527 approaches can be effective, their efficacy might be lower compared to strong chemical or
528 antibiotic treatments, especially in environments with high bacterial loads or where other
529 factors, such as nutrient availability, promote biofilm growth. Unlike chemical disinfectants,
530 which kill bacteria quickly on contact, physical antibacterial surfaces often take time to work
531 by preventing adhesion and colonisation over time, potentially limiting their effectiveness in
532 situations requiring immediate bacterial eradication.

533 Moreover, *in vivo* applications, such as implanted medical devices, introduce additional
534 challenges, such as micromotion at the tissue-implant interface, protein adsorption, and
535 inflammatory responses that may progressively alter surface architecture. The durability of
536 topographies in *in vivo* settings has yet to be extensively studied, but there is the risk of surface
537 fragmentation, which could cause the loss of antibacterial activity over time and cytotoxicity
538 to mammalian cells^{109,208}. Furthermore, surface topography may wear down due to mechanical
539 abrasion, chemical exposure, or environmental factors, leading to reduced antibacterial
540 effectiveness⁵⁹. While surface roughness can deter bacterial adhesion, excessively rough
541 surfaces might trap debris or promote biofilm accumulation in surface irregularities,
542 counteracting the intended antimicrobial effects. Ensuring consistent effectiveness may require
543 regular maintenance and monitoring. In addition, new physical antibacterial technologies may
544 face regulatory hurdles that can delay their market introduction, as they must undergo rigorous
545 testing and approval processes to meet safety and efficacy standards.

546 While physical antibacterial approaches show great potential, challenges remain in optimising
547 surface design for long-term effectiveness. Superhydrophobicity, for example, may degrade
548 due to air layer depletion, reducing its antifouling capabilities. Potential future research could
549 focus on developing robust, switchable surfaces that maintain their antibacterial properties



550 under varying environmental conditions. Additionally, further studies are needed to refine the
551 exact dimensions for maximal antibacterial efficacy while ensuring compatibility with
552 biomedical and industrial applications and processes.

553 By harnessing physical antibacterial strategies, researchers can develop innovative and
554 chemical-agent free solutions to mitigate bacterial contamination, offering promising
555 advancements in healthcare.

556

557 **5. Combination approaches**

558 Recent research suggests that the most promising route for effective and durable bacterial
559 control is the strategic combination of approaches²⁰⁹, such as surface topography with
560 chemical-based methods. While nanoscale or microscale surface structures can mechanically
561 disrupt bacterial membranes, inhibit adhesion, and delay biofilm formation, these effects alone
562 may be insufficient under complex biological or environmental conditions like healthcare
563 settings. Therefore, coupled with approaches like antibiotics, chemical disinfectants, and
564 antibacterial metals, can yield synergistic effects, enhancing both immediate bactericidal
565 activity and long-term biofilm resistance. Physical structures can reduce bacterial load and
566 delay colonisation, while potentially decreasing the dosage and frequency of chemical agents
567 ^{39,210–213}. This combined strategy not only improves performance¹¹⁷ but also helps lessen issues
568 such as toxicity and the growing concern of AMR, ultimately decreasing our reliance on
569 chemical-based interventions alone. Nonetheless, significant challenges remain, particularly
570 concerning large-scale implementation, ensuring broad-spectrum efficacy, and preventing
571 resistance that may emerge due to the inherently resilient nature of biofilms^{15,214}. More research
572 is required, but this multimodal strategy represents a promising design principle for next-
573 generation antimicrobials in healthcare settings.

574

575 **6. Conclusions**

576 Surface topography offers a promising, passive, and durable antibacterial strategy. By
577 mimicking naturally occurring antibacterial surfaces, such as insect wings or plant leaves,
578 engineered micro- and nano-scale structures can physically deter bacterial adhesion,
579 proliferation, and biofilm formation. However, the effectiveness of these topographies is highly
580 context-dependent, varying with bacterial species, surface chemistry, and environmental



581 conditions. Different bacterial species exhibit distinct adhesion behaviours and biofilm-
582 forming capacities depending on their shape, size, motility, and surface-sensing mechanisms.
583 Consequently, surface designs must be tailored to specific applications, considering the
584 dominant bacterial species likely to colonise a given medical device or environment.

585 Design strategies should also consider whether the intended outcome is antifouling (preventing
586 attachment) or bactericidal (killing adhered bacteria). For instance, antifouling surfaces may
587 be more beneficial for permanent implants to reduce biofilm formation associated with chronic
588 infection, while bactericidal topographies may be more suitable for high-risk zones where
589 sterilisation opportunities are limited. Although the antibacterial performance of such
590 biomimetic surfaces has been well documented, the underlying mechanisms of action,
591 particularly under dynamic, real-world conditions, remain an area of active research.

592 The successful implementation of topographical strategies also depends on practical and
593 engineering considerations, including scalability, fabrication precision, long-term durability,
594 and resistance to wear. Addressing these challenges requires systematic studies to develop a
595 comprehensive library of well-characterised surface architectures, mapping their effects across
596 bacterial species and environmental conditions. By first establishing a reliable experimental
597 dataset, more effective ML and AI tools can be developed.

598 The current limiting factor of predictive models of antibacterial surface topographies is the lack
599 of readily available, standardised, and high-quality datasets that capture the complexity of
600 interfaces between bacteria and the patterned surface. Current research focuses narrowly on
601 single outcome measures such as CFU counts or simple surface descriptors like roughness
602 average. In addition, many studies are conducted under static, idealised laboratory conditions,
603 often over 24 hours, which do not reflect physiologically relevant environments over time,
604 leading to limited models. It is also important to note the continually evolving and complex
605 nature of biological systems, and therefore, these datasets need to be continually updated to
606 improve the model's accuracy. These predictive technologies in turn could accelerate surface
607 design and screening, with the combination of resources helping guide the rational design of
608 application-specific surfaces for medical devices and hospital infrastructure.

609 In summary, while physical antibacterial approaches offer substantial benefits, such as reduced
610 antibiotic dependence, lower resistance risk, and sustained efficacy, they also face limitations
611 related to manufacturing complexity, cost, and maintenance. Future advances are likely to
612 emerge from dynamic surface topographies that can adapt, or combination approaches, where



613 physical topographies are combined with chemical agents such as metal-based coatings or
614 antibiotics to achieve synergistic, long-lasting protection. Translating these technologies into
615 clinical practice will require continued interdisciplinary research focused on biocompatibility,
616 long-term stability, and scalability. Ultimately, integrating topographical engineering with
617 complementary antimicrobial strategies represents a critical frontier in developing safer,
618 infection-resistant surfaces and healthcare environments.

619

620 **7. Declarations:**

621 All authors can confirm that we have no conflicts of interest to declare.

622

623 **8. Acknowledgement**

624 We would like to thank the funding support from the Medical Research Council (MRC)
625 (MR/X502972/1) Impact Acceleration Account (IAA) fund of the University of East Anglia.

626

627 **9. References**

- 628 1. Baron S. *Medical Microbiology*, 4th edition. Galveston (TX): University of Texas Medical
629 Branch at Galveston; 1996. PubMed PMID: 21413252.
- 630 2. Gupta A, Gupta R, Singh RL. *Microbes and Environment*. In: *Principles and Applications of*
631 *Environmental Biotechnology for a Sustainable Future*. Singapore: Springer Singapore; 2017.
632 p. 43–84. doi:10.1007/978-981-10-1866-4_3
- 633 3. Soni J, Sinha S, Pandey R. *Understanding bacterial pathogenicity: a closer look at the journey*
634 *of harmful microbes*. *Front Microbiol.* 2024;15:1370818. doi:10.3389/fmicb.2024.1370818
635 PubMed PMID: 38444801.
- 636 4. Zobell CE, Allen EC. *The Significance of Marine Bacteria in the Fouling of Submerged*
637 *Surfaces*. *J Bacteriol.* 1935 Mar;29(3):239–51. doi:10.1128/jb.29.3.239-251.1935
- 638 5. Zobell CE. *The Effect of Solid Surfaces upon Bacterial Activity*. *J Bacteriol.* 1943
639 Jul;46(1):39–56. doi:10.1128/jb.46.1.39-56.1943
- 640 6. Penesyan A, Paulsen IT, Kjelleberg S, Gillings MR. *Three faces of biofilms: a microbial*
641 *lifestyle, a nascent multicellular organism, and an incubator for diversity*. *NPJ Biofilms*
642 *Microbiomes.* 2021 Nov 10;7(1):80. doi:10.1038/s41522-021-00251-2
- 643 7. Sharma D, Misba L, Khan AU. *Antibiotics versus biofilm: an emerging battleground in*
644 *microbial communities*. *Antimicrob Resist Infect Control.* 2019 Dec 16;8(1):76.
645 doi:10.1186/s13756-019-0533-3



- 646 8. Nakawuki AW, Nekaka R, Ssenyonga LVN, Masifa G, Nuwasiima D, Nteziyaremye J, et al. View Article Online
DOI: 10.1039/D6LF00022C
647 Bacterial colonization, species diversity and antimicrobial susceptibility patterns of indwelling
648 urinary catheters from postpartum mothers attending a Tertiary Hospital in Eastern Uganda.
649 PLoS One. 2022 Jan 10;17(1):e0262414. doi:10.1371/journal.pone.0262414
- 650 9. van den Berg D, Asker D, Awad TS, Lavielle N, Hatton BD. Mechanical deformation of
651 elastomer medical devices can enable microbial surface colonization. *Sci Rep.* 2023 May
652 11;13(1):7691. doi:10.1038/s41598-023-34217-5
- 653 10. Bera JH, Raj A. LS, Gang S, Patel DN. Biofilm. In: *Microbial Biofilms.* Elsevier; 2023. p.
654 369–90. doi:10.1016/B978-0-323-95715-1.00010-8
- 655 11. Preda VG, Săndulescu O. Communication is the key: biofilms, quorum sensing, formation and
656 prevention. *Discoveries (Craiova).* 2019 Sep 30;7(3):e100. doi:10.15190/d.2019.13 PubMed
657 PMID: 32309618.
- 658 12. Kannan M, Rajarathinam K, Venkatesan S, Dheebe B, Maniraj A. Chapter 19 - Silver Iodide
659 Nanoparticles as an Antibiofilm Agent—A Case Study on Gram-Negative Biofilm-Forming
660 Bacteria. In: Ficaia A, Grumezescu AM, editors. *Nanostructures for Antimicrobial Therapy*
661 [Internet]. Elsevier; 2017. p. 435–56. Available from:
662 <https://www.sciencedirect.com/science/article/pii/B9780323461528000196>
663 doi:<https://doi.org/10.1016/B978-0-323-46152-8.00019-6>
- 664 13. Arunasri K, Mohan SV. Chapter 2.3 - Biofilms: Microbial Life on the Electrode Surface. In:
665 Mohan SV, Varjani S, Pandey A, editors. *Microbial Electrochemical Technology* [Internet].
666 Elsevier; 2019. p. 295–313. Available from:
667 <https://www.sciencedirect.com/science/article/pii/B978044464052900011X>
668 doi:<https://doi.org/10.1016/B978-0-444-64052-9.00011-X>
- 669 14. Shree P, Singh CK, Sodhi KK, Surya JN, Singh DK. Biofilms: Understanding the structure
670 and contribution towards bacterial resistance in antibiotics. *Medicine in Microecology.* 2023
671 Jun;16:100084. doi:10.1016/j.medmic.2023.100084
- 672 15. Zhao A, Sun J, Liu Y. Understanding bacterial biofilms: From definition to treatment
673 strategies. *Front Cell Infect Microbiol.* 2023 Apr 6;13. doi:10.3389/fcimb.2023.1137947
- 674 16. Penesyan A, Paulsen IT, Kjelleberg S, Gillings MR. Three faces of biofilms: a microbial
675 lifestyle, a nascent multicellular organism, and an incubator for diversity. *NPJ Biofilms
676 Microbiomes.* 2021 Nov 10;7(1):80. doi:10.1038/s41522-021-00251-2
- 677 17. Liu HY, Prentice EL, Webber MA. Mechanisms of antimicrobial resistance in biofilms. *npj
678 Antimicrobials and Resistance.* 2024 Oct 1;2(1):27. doi:10.1038/s44259-024-00046-3
- 679 18. Rather MA, Gupta K, Mandal M. Microbial biofilm: formation, architecture, antibiotic
680 resistance, and control strategies. *Brazilian Journal of Microbiology.* 2021 Dec 23;52(4):1701–
681 18. doi:10.1007/s42770-021-00624-x
- 682 19. Danese PN. Antibiofilm Approaches. *Chem Biol.* 2002 Aug;9(8):873–80. doi:10.1016/S1074-
683 5521(02)00192-8
- 684 20. Malheiro J, Simões M. Antimicrobial resistance of biofilms in medical devices. In: *Biofilms
685 and Implantable Medical Devices.* Elsevier; 2017. p. 97–113. doi:10.1016/B978-0-08-100382-
686 4.00004-6
- 687 21. López D, Vlamakis H, Kolter R. Biofilms. *Cold Spring Harb Perspect Biol.* 2010
688 Jul;2(7):a000398. doi:10.1101/cshperspect.a000398 PubMed PMID: 20519345.



- 689 22. Vestby LK, Grønseth T, Simm R, Nesse LL. Bacterial Biofilm and its Role in the Pathogenesis
690 of Disease. *Antibiotics*. 2020 Feb 3;9(2):59. doi:10.3390/antibiotics9020059
- 691 23. Mendhe S, Badge A, Ugemuge S, Chandi D. Impact of Biofilms on Chronic Infections and
692 Medical Challenges. *Cureus*. 2023 Nov;15(11):e48204. doi:10.7759/cureus.48204 PubMed
693 PMID: 38050493.
- 694 24. Mishra A, Aggarwal A, Khan F. Medical Device-Associated Infections Caused by Biofilm-
695 Forming Microbial Pathogens and Controlling Strategies. *Antibiotics (Basel)*. 2024 Jul
696 4;13(7). doi:10.3390/antibiotics13070623 PubMed PMID: 39061305.
- 697 25. Vestby LK, Grønseth T, Simm R, Nesse LL. Bacterial Biofilm and its Role in the Pathogenesis
698 of Disease. *Antibiotics*. 2020 Feb 3;9(2):59. doi:10.3390/antibiotics9020059
- 699 26. Ebenezer P, Kumara SPSNBS, Senevirathne SWMAI, Bray LJ, Wangchuk P, Mathew A, et al.
700 Advancements in Antimicrobial Surface Coatings Using Metal/Metaloxide Nanoparticles,
701 Antibiotics, and Phytochemicals. *Nanomaterials*. 2025 Jul 1;15(13):1023.
702 doi:10.3390/nano15131023
- 703 27. World Health Organisation. Global report on infection prevention and control 2024. Geneva:
704 World Health Organization; 2024. Licence: CC BY-NC-SA 3.0 IGO. 2024. Report.
- 705 28. Bouhrour N, Nibbering PH, Bendali F. Medical Device-Associated Biofilm Infections and
706 Multidrug-Resistant Pathogens. *Pathogens*. 2024 May 8;13(5):393.
707 doi:10.3390/pathogens13050393
- 708 29. Sharma D, Misba L, Khan AU. Antibiotics versus biofilm: an emerging battleground in
709 microbial communities. *Antimicrob Resist Infect Control*. 2019;8(1):76. doi:10.1186/s13756-
710 019-0533-3
- 711 30. Hutchings MI, Truman AW, Wilkinson B. Antibiotics: past, present and future. *Curr Opin
712 Microbiol*. 2019 Oct;51:72–80. doi:10.1016/j.mib.2019.10.008
- 713 31. Baran A, Kwiatkowska A, Potocki L. Antibiotics and Bacterial Resistance—A Short Story of
714 an Endless Arms Race. *Int J Mol Sci*. 2023 Mar 17;24(6):5777. doi:10.3390/ijms24065777
- 715 32. Salam MdA, Al-Amin MdY, Salam MT, Pawar JS, Akhter N, Rabaan AA, et al. Antimicrobial
716 Resistance: A Growing Serious Threat for Global Public Health. *Healthcare*. 2023 Jul
717 5;11(13):1946. doi:10.3390/healthcare11131946
- 718 33. Shree P, Singh CK, Sodhi KK, Surya JN, Singh DK. Biofilms: Understanding the structure
719 and contribution towards bacterial resistance in antibiotics. *Medicine in Microecology*. 2023
720 Jun;16:100084. doi:10.1016/j.medmic.2023.100084
- 721 34. Rai NK, Ashok A, Akondi BR. Consequences of chemical impact of disinfectants: safe
722 preventive measures against COVID-19. *Crit Rev Toxicol*. 2020 Jul 2;50(6):513–20.
723 doi:10.1080/10408444.2020.1790499
- 724 35. Ghafoor D, Khan Z, Khan A, Ualiyeva D, Zaman N. Excessive use of disinfectants against
725 COVID-19 posing a potential threat to living beings. *Curr Res Toxicol*. 2021;2:159–68.
726 doi:10.1016/j.crtox.2021.02.008
- 727 36. Musee N, Ngwenya P, Motaung LK, Moshuhla K, Nomngongo P. Occurrence, effects, and
728 ecological risks of chemicals in sanitizers and disinfectants: A review. *Environmental
729 Chemistry and Ecotoxicology*. 2023;5:62–78. doi:10.1016/j.enceco.2023.01.003



- 730 37. McDonnell G, Russell AD. Antiseptics and Disinfectants: Activity, Action, and Resistance. *Clin Microbiol Rev.* 1999 Jan;12(1):147–79. doi:10.1128/CMR.12.1.147
- 731
- 732 38. Pereira-Silva P, Borges J, Sampaio P. Recent advances in metal-based antimicrobial coatings. *Adv Colloid Interface Sci.* 2025 Oct;344:103590. doi:10.1016/j.cis.2025.103590
- 733
- 734 39. Birkett M, Dover L, Cherian Lukose C, Wasy Zia A, Tambuwala MM, Serrano-Aroca Á. Recent Advances in Metal-Based Antimicrobial Coatings for High-Touch Surfaces. *Int J Mol Sci.* 2022 Jan 21;23(3):1162. doi:10.3390/ijms23031162
- 735
- 736
- 737 40. Hamarawf RF. Antibacterial, antibiofilm, and antioxidant activities of two novel metal–organic frameworks (MOFs) based on 4,6-diamino-2-pyrimidinethiol with Zn and Co metal ions as coordination polymers. *RSC Adv.* 2024;14(13):9080–98. doi:10.1039/D4RA00545G
- 738
- 739
- 740 41. Huang R, Zhou Z, Lan X, Tang FK, Cheng T, Sun H, et al. Rapid synthesis of bismuth-organic frameworks as selective antimicrobial materials against microbial biofilms. *Mater Today Bio.* 2023 Feb;18:100507. doi:10.1016/j.mtbio.2022.100507
- 741
- 742
- 743 42. Sabzehmeidani MM, Kazemzad M. Recent advances in surface-mounted metal–organic framework thin film coatings for biomaterials and medical applications: a review. *Biomater Res.* 2023 Feb 9;27(1). doi:10.1186/s40824-023-00454-y
- 744
- 745
- 746 43. Rai M, Yadav A, Gade A. Silver nanoparticles as a new generation of antimicrobials. *Biotechnol Adv.* 2009 Jan;27(1):76–83. doi:10.1016/j.biotechadv.2008.09.002
- 747
- 748 44. Dwivedi S, Wahab R, Khan F, Mishra YK, Musarrat J, Al-Khedhairi AA. Reactive Oxygen Species Mediated Bacterial Biofilm Inhibition via Zinc Oxide Nanoparticles and Their Statistical Determination. *PLoS One.* 2014 Nov 17;9(11):e111289. doi:10.1371/journal.pone.0111289
- 749
- 750
- 751
- 752 45. Salah I, Parkin IP, Allan E. Copper as an antimicrobial agent: recent advances. *RSC Adv.* 2021;11(30):18179–86. doi:10.1039/D1RA02149D
- 753
- 754 46. Bisht N, Dwivedi N, Kumar P, Venkatesh M, Yadav AK, Mishra D, et al. Recent advances in copper and copper-derived materials for antimicrobial resistance and infection control. *Curr Opin Biomed Eng.* 2022 Dec;24:100408. doi:10.1016/j.cobme.2022.100408
- 755
- 756
- 757 47. Liu X, Kamperman M. Smart bacteria-responsive coatings for combating catheter-associated urinary tract infections. *Mater Today Bio.* 2025 Oct;34:102191. doi:10.1016/j.mtbio.2025.102191
- 758
- 759
- 760 48. Morgan SD, Rigby D, Stickler DJ. A study of the structure of the crystalline bacterial biofilms that can encrust and block silver Foley catheters. *Urol Res.* 2009 Apr 3;37(2):89–93. doi:10.1007/s00240-009-0176-6
- 761
- 762
- 763 49. Ortí-Lucas RM, Muñoz-Miguel J. Effectiveness of surface coatings containing silver ions in bacterial decontamination in a recovery unit. *Antimicrob Resist Infect Control.* 2017 Dec 13;6(1):61. doi:10.1186/s13756-017-0217-9
- 764
- 765
- 766 50. Wang C, Wei X, Zhong L, Chan CL, Li H, Sun H. Metal-Based Approaches for the Fight against Antimicrobial Resistance: Mechanisms, Opportunities, and Challenges. *J Am Chem Soc.* 2025 Apr 16;147(15):12361–80. doi:10.1021/jacs.4c16035
- 767
- 768
- 769 51. Shen X ting, Zhang Y zhen, Xiao F, Zhu J, Zheng X dong. Effects on cytotoxicity and antibacterial properties of the incorporations of silver nanoparticles into the surface coating of
- 770



- 771 dental alloys. *Journal of Zhejiang University-SCIENCE B*. 2017 Jul 18;18(7):615–25. [View Article Online](#)
 772 doi:10.1631/jzus.B1600555 [DOI: 10.1039/D6LF00022C](#)
- 773 52. Maillard JY, Pascoe M. Disinfectants and antiseptics: mechanisms of action and resistance.
 774 *Nat Rev Microbiol*. 2024 Jan 30;22(1):4–17. doi:10.1038/s41579-023-00958-3
- 775 53. Nunez C, Bamert RS, Lambert K, Short FL. Cleaning up our disinfectants: usage of
 776 antimicrobial biocides in direct-to-consumer products in Australia. *Access Microbiol*. 2024
 777 Feb 1;6(2). doi:10.1099/acmi.0.000714.v3
- 778 54. Graves JL. Microbial defense. In: *Principles and Applications of Antimicrobial Nanomaterials*.
 779 Elsevier; 2022. p. 137–59. doi:10.1016/B978-0-12-822105-1.00017-2
- 780 55. Andersson DI, Hughes D. Antibiotic resistance and its cost: is it possible to reverse resistance?
 781 *Nat Rev Microbiol*. 2010 Apr 8;8(4):260–71. doi:10.1038/nrmicro2319
- 782 56. O’Neill J. Antimicrobial resistance : tackling a crisis for the health and wealth of nations / the
 783 Review on Antimicrobial Resistance chaired by Jim O’Neill. Attribution 4.0 International (CC
 784 BY 4.0). Source: Wellcome Collection. 2014. Report.
- 785 57. Salam MA, Al-Amin MY, Salam MT, Pawar JS, Akhter N, Rabaan AA, et al. Antimicrobial
 786 Resistance: A Growing Serious Threat for Global Public Health. *Healthcare (Basel)*. 2023 Jul
 787 5;11(13). doi:10.3390/healthcare11131946 PubMed PMID: 37444780.
- 788 58. Murray CJL, Ikuta KS, Sharara F, Swetschinski L, Robles Aguilar G, Gray A, et al. Global
 789 burden of bacterial antimicrobial resistance in 2019: a systematic analysis. *The Lancet*. 2022
 790 Feb;399(10325):629–55. doi:10.1016/S0140-6736(21)02724-0
- 791 59. Mahanta U, Khandelwal M, Deshpande AS. Antimicrobial surfaces: a review of synthetic
 792 approaches, applicability and outlook. *J Mater Sci*. 2021;56(32):17915–41.
 793 doi:10.1007/s10853-021-06404-0
- 794 60. Sheridan M, Winters C, Zamboni F, Collins MN. Biomaterials: Antimicrobial surfaces in
 795 biomedical engineering and healthcare. *Curr Opin Biomed Eng*. 2022 Jun;22:100373.
 796 doi:10.1016/j.cobme.2022.100373
- 797 61. Su Q, Xue Y, Wang C, Zhou Q, Zhao Y, Su J, et al. Strategies and applications of antibacterial
 798 surface-modified biomaterials. *Bioact Mater*. 2025 Nov;53:114–40.
 799 doi:10.1016/j.bioactmat.2025.07.009
- 800 62. Fernandes S, Gomes IB, Simões M, Simões LC. Novel chemical-based approaches for biofilm
 801 cleaning and disinfection. *Curr Opin Food Sci*. 2024 Feb;55:101124.
 802 doi:10.1016/j.cofs.2024.101124
- 803 63. Chung KK, Schumacher JF, Sampson EM, Burne RA, Antonelli PJ, Brennan AB. Impact of
 804 engineered surface microtopography on biofilm formation of *Staphylococcus aureus*.
 805 *Biointerphases*. 2007 Jun;2(2):89–94. doi:10.1116/1.2751405
- 806 64. Tiller JC, Liao CJ, Lewis K, Klivanov AM. Designing surfaces that kill bacteria on contact.
 807 *Proceedings of the National Academy of Sciences*. 2001 May 22;98(11):5981–5.
 808 doi:10.1073/pnas.111143098
- 809 65. Ivanova EP, Truong VK, Webb HK, Baulin VA, Wang JY, Mohammadi N, et al. Differential
 810 attraction and repulsion of *Staphylococcus aureus* and *Pseudomonas aeruginosa* on
 811 molecularly smooth titanium films. *Sci Rep*. 2011 Nov 22;1(1):165. doi:10.1038/srep00165



- 812 66. Mrabet B, Nguyen MN, Majbri A, Mahouche S, Turmine M, Bakhrouf A, et al. Anti-fouling
813 poly(2-hydroxyethyl methacrylate) surface coatings with specific bacteria recognition
814 capabilities. *Surf Sci.* 2009 Aug;603(16):2422–9. doi:10.1016/j.susc.2009.05.020
- 815 67. Ivanova EP, Hasan J, Webb HK, Truong VK, Watson GS, Watson JA, et al. Natural
816 Bactericidal Surfaces: Mechanical Rupture of *Pseudomonas aeruginosa* Cells by Cicada
817 Wings. *Small.* 2012 Aug 20;8(16):2489–94. doi:10.1002/smll.201200528
- 818 68. Elbourne A, Crawford RJ, Ivanova EP. Nano-structured antimicrobial surfaces: From nature to
819 synthetic analogues. *J Colloid Interface Sci.* 2017 Dec;508:603–16.
820 doi:10.1016/j.jcis.2017.07.021
- 821 69. Barthlott W, Neinhuis C. Purity of the sacred lotus, or escape from contamination in biological
822 surfaces. *Planta.* 1997;202(1):1–8. doi:10.1007/s004250050096
- 823 70. Ivanova EP, Hasan J, Webb HK, Truong VK, Watson GS, Watson JA, et al. Natural
824 Bactericidal Surfaces: Mechanical Rupture of *Pseudomonas aeruginosa* Cells by Cicada
825 Wings. *Small.* 2012 Aug 20;8(16):2489–94. doi:10.1002/smll.201200528
- 826 71. Liu K, Jiang L. Bio-inspired design of multiscale structures for function integration. *Nano*
827 *Today.* 2011 Apr;6(2):155–75. doi:10.1016/j.nantod.2011.02.002
- 828 72. Velic A, Hasan J, Li Z, Yarlagadda PKD V. Mechanics of Bacterial Interaction and Death on
829 Nanopatterned Surfaces. *Biophys J.* 2021 Jan 19;120(2):217–31.
830 doi:10.1016/j.bpj.2020.12.003
- 831 73. Chien HW, Chen XY, Tsai WP, Lee M. Inhibition of biofilm formation by rough shark skin-
832 patterned surfaces. *Colloids Surf B Biointerfaces.* 2020 Feb;186:110738.
833 doi:10.1016/j.colsurfb.2019.110738
- 834 74. Tian G, Fan D, Feng X, Zhou H. Thriving artificial underwater drag-reduction materials
835 inspired from aquatic animals: progresses and challenges. *RSC Adv.* 2021;11(6):3399–428.
836 doi:10.1039/D0RA08672J
- 837 75. Mann EE, Manna D, Mettetal MR, May RM, Dannemiller EM, Chung KK, et al. Surface
838 micropattern limits bacterial contamination. *Antimicrob Resist Infect Control.* 2014;3(1):28.
839 doi:10.1186/2047-2994-3-28
- 840 76. Liu Q, Brookbank L, Ho A, Coffey J, Brennan AB, Jones CJ. Surface texture limits transfer of
841 *S. aureus*, T4 Bacteriophage, Influenza B virus and Human coronavirus. 2020.
842 doi:10.1101/2020.09.10.20192351
- 843 77. Reddy ST, Chung KK, McDaniel CJ, Darouiche RO, Landman J, Brennan AB. Micropatterned
844 Surfaces for Reducing the Risk of Catheter-Associated Urinary Tract Infection: An *In Vitro*
845 Study on the Effect of Sharklet Micropatterned Surfaces to Inhibit Bacterial Colonization and
846 Migration of Uropathogenic *Escherichia coli*. *J Endourol.* 2011 Sep;25(9):1547–52.
847 doi:10.1089/end.2010.0611
- 848 78. Arango-Santander S. Bioinspired Topographic Surface Modification of Biomaterials.
849 *Materials.* 2022 Mar 24;15(7):2383. doi:10.3390/ma15072383
- 850 79. Redfern J, Cunliffe AJ, Goeres DM, Azevedo NF, Verran J. Critical analysis of methods to
851 determine growth, control and analysis of biofilms for potential non-submerged antibiofilm
852 surfaces and coatings. *Biofilm.* 2024 Jun;7:100187. doi:10.1016/j.biofilm.2024.100187



- 853 80. Li L, Mendis N, Trigui H, Oliver JD, Faucher SP. The importance of the viable but non-
 854 culturable state in human bacterial pathogens. *Front Microbiol.* 2014 Jun 2;5. View Article Online
 855 doi:10.3389/fmicb.2014.00258 DOI: 10.1039/D6LF00022C
- 856 81. Haney E, Trimble M, Cheng J, Vallé Q, Hancock R. Critical Assessment of Methods to
 857 Quantify Biofilm Growth and Evaluate Antibiofilm Activity of Host Defence Peptides.
 858 *Biomolecules.* 2018 May 21;8(2):29. doi:10.3390/biom8020029
- 859 82. Meyer CT, Lynch GK, Stamo DF, Miller EJ, Chatterjee A, Kralj JM. A high-throughput and
 860 low-waste viability assay for microbes. *Nat Microbiol.* 2023 Nov 2;8(12):2304–14.
 861 doi:10.1038/s41564-023-01513-9
- 862 83. Martini KM, Boddu SS, Nemenman I, Vega NM. Maximum likelihood estimators for colony-
 863 forming units. *Microbiol Spectr.* 2024 Sep 3;12(9). doi:10.1128/spectrum.03946-23
- 864 84. Gerardi D, Bernardi S, Bruni A, Falisi G, Botticelli G. Characterization and morphological
 865 methods for oral biofilm visualization: where are we nowadays? *AIMS Microbiol.*
 866 2024;10(2):391–414. doi:10.3934/microbiol.2024020
- 867 85. Awadh AA, Kelly AF, Forster-Wilkins G, Wertheim D, Giddens R, Gould SW, et al.
 868 Visualisation and biovolume quantification in the characterisation of biofilm formation in
 869 *Mycoplasma fermentans.* *Sci Rep.* 2021 May 27;11(1):11259. doi:10.1038/s41598-021-90455-
 870 5
- 871 86. Nishida T, Seino S, Imoto Y. Visualizing Antimicrobial Effects on Bacterial Surfaces by
 872 <sc>SEM</sc> : A Comparative Study of Hexamethyldisilazane (<sc>HMDS</sc>)
 873 and Freeze-Drying. *Microsc Res Tech.* 2025 Dec 27;88(12):3273–81. doi:10.1002/jemt.70037
- 874 87. Rosenberg M, Azevedo NF, Ivask A. Propidium iodide staining underestimates viability of
 875 adherent bacterial cells. *Sci Rep.* 2019 Apr 24;9(1):6483. doi:10.1038/s41598-019-42906-3
- 876 88. Stiefel P, Schmidt-Emrich S, Maniura-Weber K, Ren Q. Critical aspects of using bacterial cell
 877 viability assays with the fluorophores SYTO9 and propidium iodide. *BMC Microbiol.* 2015
 878 Dec 18;15(1):36. doi:10.1186/s12866-015-0376-x
- 879 89. Tchatchiashvili T, Jundzill M, Marquet M, Mirza KA, Pletz MW, Makarewicz O, et al.
 880 CAM/TMA-DPH as a promising alternative to SYTO9/PI for cell viability assessment in
 881 bacterial biofilms. *Front Cell Infect Microbiol.* 2025 Jan 21;14.
 882 doi:10.3389/fcimb.2024.1508016
- 883 90. Netuschil L, Ausschil TM, Sculean A, Arweiler NB. Confusion over live/dead stainings for the
 884 detection of vital microorganisms in oral biofilms - which stain is suitable? *BMC Oral Health.*
 885 2014 Dec 11;14(1):2. doi:10.1186/1472-6831-14-2
- 886 91. Raab N, Bachelet I. Resolving biofilm topography by native scanning electron microscopy. *J*
 887 *Biol Methods.* 2024 Apr 25;4(2):1. doi:10.14440/jbm.2017.173
- 888 92. Kumar M, Bhardwaj R. Wetting characteristics of *Colocasia esculenta* (Taro) leaf and a
 889 bioinspired surface thereof. *Sci Rep.* 2020 Jan 22;10(1):935. doi:10.1038/s41598-020-57410-2
- 890 93. Cates N, Einck VJ, Micklow L, Morère J, Okoroanyanwu U, Watkins JJ, et al. Roll-to-roll
 891 nanoimprint lithography using a seamless cylindrical mold nanopatterned with a high-speed
 892 mastering process. *Nanotechnology.* 2021 Apr 9;32(15):155301. doi:10.1088/1361-
 893 6528/abd9f1



- 894 94. Kooy N, Mohamed K, Pin LT, Guan OS. A review of roll-to-roll nanoimprint lithography. *Nanoscale Res Lett.* 2014 Dec 25;9(1):320. doi:10.1186/1556-276X-9-320 View Article Online
DOI: 10.1039/D6LF00022C
- 895
- 896 95. Dundar Arisoy F, Kolewe KW, Homyak B, Kurtz IS, Schiffman JD, Watkins JJ. Bioinspired
897 Photocatalytic Shark-Skin Surfaces with Antibacterial and Antifouling Activity via
898 Nanoimprint Lithography. *ACS Appl Mater Interfaces.* 2018 Jun 13;10(23):20055–63.
899 doi:10.1021/acsami.8b05066
- 900 96. Du C, Wang C, Zhang T, Zheng L. Antibacterial Performance of Zr-BMG, Stainless Steel, and
901 Titanium Alloy with Laser-Induced Periodic Surface Structures. *ACS Appl Bio Mater.* 2022
902 Jan 17;5(1):272–84. doi:10.1021/acsabm.1c01075
- 903 97. Bonse J, Kirner S V, Krüger J. Laser-Induced Periodic Surface Structures (LIPSS). In:
904 Sugioka K, editor. *Handbook of Laser Micro- and Nano-Engineering* [Internet]. Cham:
905 Springer International Publishing; 2020. p. 1–59. Available from: https://doi.org/10.1007/978-3-319-69537-2_17-1 doi:10.1007/978-3-319-69537-2_17-1
- 906
- 907 98. Grossmann S, Tetzlaff L, Grabow N, Schmitz KP, Siewert S. LIPSS on polymeric implant
908 surfaces - a fabrication study. *Current Directions in Biomedical Engineering.* 2024 Dec
909 1;10(4):280–3. doi:10.1515/cdbme-2024-2068
- 910 99. Gupta R, Gaddam A, Prajapati D, Dimov S, Mishra A, Vadali M. Enhancing Bactericidal
911 Properties of Ti6Al4V Surfaces through Micro and Nano Hierarchical Laser Texturing.
912 *Langmuir.* 2024 Aug 13;40(32):16791–803. doi:10.1021/acs.langmuir.4c01173
- 913 100. Oubellaouch K, Orazi L, Brun P, Lucchetta G, Pelaccia R, Sorgato M. An innovative process
914 chain for the production of antibiofouling polymer parts using ultrafast laser texturing. *The
915 International Journal of Advanced Manufacturing Technology.* 2024 Sep 6.
916 doi:10.1007/s00170-024-14369-y
- 917 101. Lozano-Hernández N, Pérez Llanos G, Saez Comet C, del Valle LJ, Puiggali J, Fontdecaba E.
918 Micro- and Nanotexturization of Liquid Silicone Rubber Surfaces by Injection Molding Using
919 Hybrid Polymer Inlays. *Macromol Mater Eng.* 2022 Mar 24;307(3).
920 doi:10.1002/mame.202100741
- 921 102. Jaggessar A, Shahali H, Mathew A, Yarlagadda PKD V. Bio-mimicking nano and micro-
922 structured surface fabrication for antibacterial properties in medical implants. *J
923 Nanobiotechnology.* 2017 Dec 2;15(1):64. doi:10.1186/s12951-017-0306-1
- 924 103. Yadav SK, Aravindan S, Rao P V. Characterisation of micro-textures created by hot
925 embossing on polystyrene for probable use as an antireflective coating. *Surface Engineering.*
926 2025 Mar 28;41(3):403–16. doi:10.1177/02670844251321586
- 927 104. Ivanova EP, Hasan J, Webb HK, Gervinskas G, Juodkazis S, Truong VK, et al. Bactericidal
928 activity of black silicon. *Nat Commun.* 2013 Nov 26;4(1):2838. doi:10.1038/ncomms3838
- 929 105. Benčina M, Resnik M, Starič P, Junkar I. Use of Plasma Technologies for Antibacterial
930 Surface Properties of Metals. *Molecules.* 2021 Mar 5;26(5):1418.
931 doi:10.3390/molecules26051418
- 932 106. Asadi Tokmedash M, Kim C, Chavda AP, Li A, Robins J, Min J. Engineering multifunctional
933 surface topography to regulate multiple biological responses. *Biomaterials.* 2025
934 Aug;319:123136. doi:10.1016/j.biomaterials.2025.123136



- 935 107. Yang F, Pan Z, Shen L, Huang D, Gao H, Wang X, et al. Recent advances in marine
936 biomimetic antifouling technology based on microstructured surfaces inspired by aquatic
937 organisms. *J Coat Technol Res.* 2026 Feb 17. doi:10.1007/s11998-025-01219-z View Article Online
DOI: 10.1039/D6LF00022C
- 938 108. Francone A, Merino S, Retolaza A, Ramiro J, Alves SA, de Castro JV, et al. Impact of surface
939 topography on the bacterial attachment to micro- and nano-patterned polymer films. *Surfaces
940 and Interfaces.* 2021 Dec;27:101494. doi:10.1016/j.surfin.2021.101494
- 941 109. Ishak MI, Liu X, Jenkins J, Nobbs AH, Su B. Protruding Nanostructured Surfaces for
942 Antimicrobial and Osteogenic Titanium Implants. *Coatings.* 2020 Aug 3;10(8):756.
943 doi:10.3390/coatings10080756
- 944 110. Jiang R, Hao L, Song L, Tian L, Fan Y, Zhao J, et al. Lotus-leaf-inspired hierarchical
945 structured surface with non-fouling and mechanical bactericidal performances. *Chemical
946 Engineering Journal.* 2020 Oct;398:125609. doi:10.1016/j.cej.2020.125609
- 947 111. Moran JA, Hawkins BJ, Gowen BE, Robbins SL. Ion fluxes across the pitcher walls of three
948 Bornean Nepenthes pitcher plant species: flux rates and gland distribution patterns reflect
949 nitrogen sequestration strategies. *J Exp Bot.* 2010 Mar 1;61(5):1365–74.
950 doi:10.1093/jxb/erq004
- 951 112. Kamarajan BP, Muthusamy A. Survival strategy of *Pseudomonas aeruginosa* on the nanopillar
952 topography of dragonfly (*Pantala flavescens*) wing. *AMB Express.* 2020 Dec 6;10(1):85.
953 doi:10.1186/s13568-020-01021-7
- 954 113. Pogodin S, Hasan J, Baulin VA, Webb HK, Truong VK, Phong Nguyen TH, et al. Biophysical
955 Model of Bacterial Cell Interactions with Nanopatterned Cicada Wing Surfaces. *Biophys J.*
956 2013 Feb;104(4):835–40. doi:10.1016/j.bpj.2012.12.046
- 957 114. Watson GS, Green DW, Schwarzkopf L, Li X, Cribb BW, Myhra S, et al. A gecko skin
958 micro/nano structure – A low adhesion, superhydrophobic, anti-wetting, self-cleaning,
959 biocompatible, antibacterial surface. *Acta Biomater.* 2015 Jul;21:109–22.
960 doi:10.1016/j.actbio.2015.03.007
- 961 115. Yang M, Ding Y, Ge X, Leng Y. Control of bacterial adhesion and growth on honeycomb-like
962 patterned surfaces. *Colloids Surf B Biointerfaces.* 2015 Nov;135:549–55.
963 doi:10.1016/j.colsurfb.2015.08.010
- 964 116. Elbourne A, Coyle VE, Truong VK, Sabri YM, Kandjani AE, Bhargava SK, et al. Multi-
965 directional electrodeposited gold nanospikes for antibacterial surface applications. *Nanoscale
966 Adv.* 2019;1(1):203–12. doi:10.1039/C8NA00124C
- 967 117. Khursheed A, Xu L, Siedlecki CA. The effects of submicron-textured surface topography on
968 antibiotic efficacy against biofilms. *J Biomed Mater Res B Appl Biomater.* 2024 Jul 3;112(7).
969 doi:10.1002/jbm.b.35436
- 970 118. Singh A, Yoon ES. Biomimetics in Tribology - Recent Developments. *Journal of The Korean
971 Physical Society - J KOREAN PHYS SOC.* 2008 Mar 15;52. doi:10.3938/jkps.52.656
- 972 119. Latthe S, Terashima C, Nakata K, Fujishima A. Superhydrophobic Surfaces Developed by
973 Mimicking Hierarchical Surface Morphology of Lotus Leaf. *Molecules.* 2014 Apr
974 4;19(4):4256–83. doi:10.3390/molecules19044256
- 975 120. Zhao A, Sun J, Liu Y. Understanding bacterial biofilms: From definition to treatment
976 strategies. *Front Cell Infect Microbiol.* 2023 Apr 6;13. doi:10.3389/fcimb.2023.1137947



- 977 121. Ma J, Sun Y, Gleichauf K, Lou J, Li Q. Nanostructure on Taro Leaves Resists Fouling by View Article Online
DOI: 10.1039/D6LF00022C
978 Colloids and Bacteria under Submerged Conditions. *Langmuir*. 2011 Aug 16;27(16):10035–
979 40. doi:10.1021/la2010024
- 980 122. Rajab FH, Liauw CM, Benson PS, Li L, Whitehead KA. Production of hybrid
981 macro/micro/nano surface structures on Ti6Al4V surfaces by picosecond laser surface
982 texturing and their antifouling characteristics. *Colloids Surf B Biointerfaces*. 2017
983 Dec;160:688–96. doi:10.1016/j.colsurfb.2017.10.008
- 984 123. Ankhelyi M V., Wainwright DK, Lauder G V. Diversity of dermal denticle structure in sharks:
985 Skin surface roughness and three-dimensional morphology. *J Morphol*. 2018 Aug
986 29;279(8):1132–54. doi:10.1002/jmor.20836
- 987 124. Kelleher SM, Habimana O, Lawler J, O' Reilly B, Daniels S, Casey E, et al. Cicada Wing
988 Surface Topography: An Investigation into the Bactericidal Properties of Nanostructural
989 Features. *ACS Appl Mater Interfaces*. 2016 Jun 22;8(24):14966–74.
990 doi:10.1021/acsami.5b08309
- 991 125. Kelleher SM, Habimana O, Lawler J, O' Reilly B, Daniels S, Casey E, et al. Cicada Wing
992 Surface Topography: An Investigation into the Bactericidal Properties of Nanostructural
993 Features. *ACS Appl Mater Interfaces*. 2016 Jun 22;8(24):14966–74.
994 doi:10.1021/acsami.5b08309
- 995 126. Ivanova EP, Hasan J, Webb HK, Gervinskias G, Juodkazis S, Truong VK, et al. Bactericidal
996 activity of black silicon. *Nat Commun*. 2013 Nov 26;4(1):2838. doi:10.1038/ncomms3838
- 997 127. Bandara CD, Singh S, Afara IO, Wolff A, Tesfamichael T, Ostrikov K, et al. Bactericidal
998 Effects of Natural Nanotopography of Dragonfly Wing on *Escherichia coli*. *ACS Appl Mater*
999 *Interfaces*. 2017 Mar 1;9(8):6746–60. doi:10.1021/acsami.6b13666
- 1000 128. Mainwaring DE, Nguyen SH, Webb H, Jakubov T, Tobin M, Lamb RN, et al. The nature of
1001 inherent bactericidal activity: insights from the nanotopology of three species of dragonfly.
1002 *Nanoscale*. 2016;8(12):6527–34. doi:10.1039/C5NR08542J
- 1003 129. Linklater DP, Juodkazis S, Crawford RJ, Ivanova EP. Mechanical inactivation of
1004 *Staphylococcus aureus* and *Pseudomonas aeruginosa* by titanium substrata with hierarchical
1005 surface structures. *Materialia (Oxf)*. 2019 Mar;5:100197. doi:10.1016/j.mtla.2018.100197
- 1006 130. Li W, Thian ES, Wang M, Wang Z, Ren L. Surface Design for Antibacterial Materials: From
1007 Fundamentals to Advanced Strategies. *Advanced Science*. 2021 Oct 5;8(19).
1008 doi:10.1002/advs.202100368
- 1009 131. Truong VK, Geeganagamage NM, Baulin VA, Vongsvivut J, Tobin MJ, Luque P, et al. The
1010 susceptibility of *Staphylococcus aureus* CIP 65.8 and *Pseudomonas aeruginosa* ATCC 9721
1011 cells to the bactericidal action of nanostructured *Calopteryx haemorrhoidalis* damselfly wing
1012 surfaces. *Appl Microbiol Biotechnol*. 2017;101(11):4683–90. doi:10.1007/s00253-017-8205-9
- 1013 132. Linklater DP, Baulin VA, Le Guével X, Fleury J, Hanssen E, Nguyen THP, et al. Antibacterial
1014 Action of Nanoparticles by Lethal Stretching of Bacterial Cell Membranes. *Advanced*
1015 *Materials*. 2020 Dec 12;32(52). doi:10.1002/adma.202005679
- 1016 133. Hazell G, May PW, Taylor P, Nobbs AH, Welch CC, Su B. Studies of black silicon and black
1017 diamond as materials for antibacterial surfaces. *Biomater Sci*. 2018;6(6):1424–32.
1018 doi:10.1039/C8BM00107C



- 1019 134. Modaresifar K, Azizian S, Ganjian M, Fratila-Apachitei LE, Zadpoor AA. Bactericidal effects
 1020 of nanopatterns: A systematic review. *Acta Biomater.* 2019 Jan;83:29–36.
 1021 doi:10.1016/j.actbio.2018.09.059
- 1022 135. Ivanova EP, Hasan J, Webb HK, Gervinskis G, Juodkazis S, Truong VK, et al. Bactericidal
 1023 activity of black silicon. *Nat Commun.* 2013 Nov 26;4(1):2838. doi:10.1038/ncomms3838
- 1024 136. Mu M, Liu S, DeFlorio W, Hao L, Wang X, Salazar KS, et al. Influence of Surface
 1025 Roughness, Nanostructure, and Wetting on Bacterial Adhesion. *Langmuir.* 2023 Apr
 1026 18;39(15):5426–39. doi:10.1021/acs.langmuir.3c00091
- 1027 137. Perera-Costa D, Bruque JM, González-Martín ML, Gómez-García AC, Vadillo-Rodríguez V.
 1028 Studying the Influence of Surface Topography on Bacterial Adhesion using Spatially
 1029 Organized Microtopographic Surface Patterns. *Langmuir.* 2014 Apr 29;30(16):4633–41.
 1030 doi:10.1021/la5001057
- 1031 138. Mu M, Liu S, DeFlorio W, Hao L, Wang X, Salazar KS, et al. Influence of Surface
 1032 Roughness, Nanostructure, and Wetting on Bacterial Adhesion. *Langmuir.* 2023 Apr
 1033 18;39(15):5426–39. doi:10.1021/acs.langmuir.3c00091
- 1034 139. Tripathy A, Sen P, Su B, Briscoe WH. Natural and bioinspired nanostructured bactericidal
 1035 surfaces. *Adv Colloid Interface Sci.* 2017;248:85–104.
 1036 doi:https://doi.org/10.1016/j.cis.2017.07.030
- 1037 140. Hasan J, Raj S, Yadav L, Chatterjee K. Engineering a nanostructured “super surface” with
 1038 superhydrophobic and superkilling properties. *RSC Adv.* 2015;5(56):44953–9.
 1039 doi:10.1039/C5RA05206H
- 1040 141. Linklater DP, Nguyen HKD, Bhadra CM, Juodkazis S, Ivanova EP. Influence of nanoscale
 1041 topology on bactericidal efficiency of black silicon surfaces. *Nanotechnology.* 2017 Jun
 1042 16;28(24):245301. doi:10.1088/1361-6528/aa700e
- 1043 142. May PW, Clegg M, Silva TA, Zanin H, Fatibello-Filho O, Celorrio V, et al. Diamond-coated
 1044 ‘black silicon’ as a promising material for high-surface-area electrochemical electrodes and
 1045 antibacterial surfaces. *J Mater Chem B.* 2016;4(34):5737–46. doi:10.1039/C6TB01774F
- 1046 143. Fisher LE, Yang Y, Yuen MF, Zhang W, Nobbs AH, Su B. Bactericidal activity of biomimetic
 1047 diamond nanocone surfaces. *Biointerphases.* 2016 Mar 1;11(1). doi:10.1116/1.4944062
- 1048 144. Bhadra CM, Khanh Truong V, Pham VTH, Al Kobaisi M, Seniutinas G, Wang JY, et al.
 1049 Antibacterial titanium nano-patterned arrays inspired by dragonfly wings. *Sci Rep.* 2015 Nov
 1050 18;5(1):16817. doi:10.1038/srep16817
- 1051 145. Sengstock C, Lopian M, Motemani Y, Borgmann A, Khare C, Buenconsejo PJS, et al.
 1052 Structure-related antibacterial activity of a titanium nanostructured surface fabricated by
 1053 glancing angle sputter deposition. *Nanotechnology.* 2014 May 16;25(19):195101.
 1054 doi:10.1088/0957-4484/25/19/195101
- 1055 146. Hizal F, Zhuk I, Sukhishvili S, Busscher HJ, van der Mei HC, Choi CH. Impact of 3D
 1056 Hierarchical Nanostructures on the Antibacterial Efficacy of a Bacteria-Triggered Self-
 1057 Defensive Antibiotic Coating. *ACS Appl Mater Interfaces.* 2015 Sep 16;7(36):20304–13.
 1058 doi:10.1021/acsami.5b05947
- 1059 147. Sjöström T, Nobbs AH, Su B. Bactericidal nanospine surfaces via thermal oxidation of Ti
 1060 alloy substrates. *Mater Lett.* 2016 Mar;167:22–6. doi:10.1016/j.matlet.2015.12.140



- 1061 148. Diu T, Faruqui N, Sjöström T, Lamarre B, Jenkinson HF, Su B, et al. Cicada-inspired cell-instructive nanopatterned arrays. *Sci Rep.* 2014 Nov 20;4(1):7122. doi:10.1038/srep07122 View Article Online
DOI: 10.1039/D6LF00022C
- 1063 149. Ge X, Ren C, Ding Y, Chen G, Lu X, Wang K, et al. Micro/nano-structured TiO₂ surface with dual-functional antibacterial effects for biomedical applications. *Bioact Mater.* 2019 Dec;4:346–57. doi:10.1016/j.bioactmat.2019.10.006
- 1066 150. Hasan J, Xu Y, Yarlagadda T, Schuetz M, Spann K, Yarlagadda PK. Antiviral and Antibacterial Nanostructured Surfaces with Excellent Mechanical Properties for Hospital Applications. *ACS Biomater Sci Eng.* 2020 Jun 8;6(6):3608–18. doi:10.1021/acsbiomaterials.0c00348
- 1070 151. Dickson MN, Liang EI, Rodriguez LA, Vollereaux N, Yee AF. Nanopatterned polymer surfaces with bactericidal properties. *Biointerphases.* 2015 Jun;10(2):021010. doi:10.1116/1.4922157
- 1073 152. Nerantzaki M, Kehagias N, Francone A, Fernández A, Sotomayor Torres CM, Papi R, et al. Design of a Multifunctional Nanoengineered PLLA Surface by Maximizing the Synergies between Biochemical and Surface Design Bactericidal Effects. *ACS Omega.* 2018 Feb 28;3(2):1509–21. doi:10.1021/acsomega.7b01756
- 1077 153. Cui Q, Liu T, Li X, Song K, Ge D. Nanopillared Polycarbonate Surfaces Having Variable Feature Parameters as Bactericidal Coatings. *ACS Appl Nano Mater.* 2020 May 22;3(5):4599–609. doi:10.1021/acsanm.0c00645
- 1080 154. Green DW, Lee KKH, Watson JA, Kim HY, Yoon KS, Kim EJ, et al. High Quality Bioreplication of Intricate Nanostructures from a Fragile Gecko Skin Surface with Bactericidal Properties. *Sci Rep.* 2017 Jan 25;7(1):41023. doi:10.1038/srep41023
- 1083 155. Wu S, Zuber F, Brugger J, Maniura-Weber K, Ren Q. Antibacterial Au nanostructured surfaces. *Nanoscale.* 2016;8(5):2620–5. doi:10.1039/C5NR06157A
- 1085 156. Alameda MT, Osorio MR, Hernández JJ, Rodríguez I. Hierarchical micro-nano topographies to control Bacteria and mesenchymal stem cells biological responses. *Sci Rep.* 2025 Jul 14;15(1):25405. doi:10.1038/s41598-025-08415-2
- 1088 157. Kargar M, Pruden A, Ducker WA. Preventing bacterial colonization using colloidal crystals. *J Mater Chem B.* 2014;2(36):5962–71. doi:10.1039/C4TB00835A
- 1090 158. Feng G, Cheng Y, Wang SY, Borca-Tasciuc DA, Worobo RW, Moraru CI. Bacterial attachment and biofilm formation on surfaces are reduced by small-diameter nanoscale pores: how small is small enough? *NPJ Biofilms Microbiomes.* 2015 Dec 2;1(1):15022. doi:10.1038/npjbiofilms.2015.22
- 1094 159. Hsieh PC, Chien HW. Biomimetic surfaces: Insights on the role of surface topography and wetting properties in bacterial attachment and biofilm formation. *Colloids Surf B Biointerphases.* 2023 Aug;228:113389. doi:10.1016/j.colsurfb.2023.113389
- 1097 160. Mok R, Dunkel J, Kantsler V. Geometric control of bacterial surface accumulation. *Phys Rev E.* 2019 May 24;99(5):052607. doi:10.1103/PhysRevE.99.052607
- 1099 161. Gu H, Kolewe KW, Ren D. Conjugation in *Escherichia coli* Biofilms on Poly(dimethylsiloxane) Surfaces with Microtopographic Patterns. *Langmuir.* 2017 Mar 28;33(12):3142–50. doi:10.1021/acs.langmuir.6b04679



- 1102 162. Gu H, Chen A, Song X, Brasch ME, Henderson JH, Ren D. How *Escherichia coli* lands and
 1103 forms cell clusters on a surface: a new role of surface topography. *Sci Rep*. 2016 Jul
 1104 14;6(1):29516. doi:10.1038/srep29516
- 1105 163. Linklater DP, Baulin VA, Juodkakis S, Crawford RJ, Stoodley P, Ivanova EP. Mechano-
 1106 bactericidal actions of nanostructured surfaces. *Nat Rev Microbiol*. 2021;19(1):8–22.
 1107 doi:10.1038/s41579-020-0414-z
- 1108 164. Wijethunge D, Mathew A, Yarlagadda PKD V. Comprehensive review of bacterial death
 1109 mechanism on nanopillared nanostructured surfaces. *Biophys Rev*. 2025 Jun 20;17(3):893–
 1110 908. doi:10.1007/s12551-025-01319-5
- 1111 165. Linklater DP, Ivanova EP. Nanostructured antibacterial surfaces – What can be achieved?
 1112 *Nano Today*. 2022 Apr;43:101404. doi:10.1016/j.nantod.2022.101404
- 1113 166. Uneputti A, Dávila-Lezama A, Garibo D, Oknianska A, Bogdanchikova N, Hernández-
 1114 Sánchez JF, et al. Strategies applied to modify structured and smooth surfaces: A step closer to
 1115 reduce bacterial adhesion and biofilm formation. *Colloid Interface Sci Commun*. 2022
 1116 Jan;46:100560. doi:10.1016/j.colcom.2021.100560
- 1117 167. Wu S, Zuber F, Maniura-Weber K, Brugger J, Ren Q. Nanostructured surface topographies
 1118 have an effect on bactericidal activity. *J Nanobiotechnology*. 2018 Dec 28;16(1):20.
 1119 doi:10.1186/s12951-018-0347-0
- 1120 168. Zhang X, Wang L, Levänen E. Superhydrophobic surfaces for the reduction of bacterial
 1121 adhesion. *RSC Adv*. 2013;3(30):12003. doi:10.1039/c3ra40497h
- 1122 169. Drelich J, Chibowski E, Meng DD, Terpilowski K. Hydrophilic and superhydrophilic surfaces
 1123 and materials. *Soft Matter*. 2011;7(21):9804. doi:10.1039/c1sm05849e
- 1124 170. Hizal F, Rungraeng N, Lee J, Jun S, Busscher HJ, van der Mei HC, et al. Nanoengineered
 1125 Superhydrophobic Surfaces of Aluminum with Extremely Low Bacterial Adhesivity. *ACS*
 1126 *Appl Mater Interfaces*. 2017 Apr 5;9(13):12118–29. doi:10.1021/acsami.7b01322
- 1127 171. Ellinas K, Kefallinou D, Stamatakis K, Gogolides E, Tserepi A. Is There a Threshold in the
 1128 Antibacterial Action of Superhydrophobic Surfaces? *ACS Appl Mater Interfaces*. 2017 Nov
 1129 15;9(45):39781–9. doi:10.1021/acsami.7b11402
- 1130 172. Rutherford ST, Bassler BL. Bacterial Quorum Sensing: Its Role in Virulence and Possibilities
 1131 for Its Control. *Cold Spring Harb Perspect Med*. 2012 Nov 1;2(11):a012427–a012427.
 1132 doi:10.1101/cshperspect.a012427
- 1133 173. Cuahtecontzi Delint R, Ishak MI, Tsimbouri PM, Jayawarna V, Burgess KVE, Ramage G, et
 1134 al. Nanotopography Influences Host–Pathogen Quorum Sensing and Facilitates Selection of
 1135 Bioactive Metabolites in Mesenchymal Stromal Cells and *Pseudomonas aeruginosa* Co-
 1136 Cultures. *ACS Appl Mater Interfaces*. 2024 Aug 21;16(33):43374–86.
 1137 doi:10.1021/acsami.4c09291
- 1138 174. Romero M, Luckett J, Dubern JF, Figueredo GP, Ison E, Carabelli AM, et al. Combinatorial
 1139 discovery of microtopographical landscapes that resist biofilm formation through quorum
 1140 sensing mediated autolubrication. *Nat Commun*. 2025 Jun 18;16(1):5295. doi:10.1038/s41467-
 1141 025-60567-x
- 1142 175. Mukherjee S, Bassler BL. Bacterial quorum sensing in complex and dynamically changing
 1143 environments. *Nat Rev Microbiol*. 2019 Jun 3;17(6):371–82. doi:10.1038/s41579-019-0186-5



- 1144 176. Mishra A, Aggarwal A, Khan F. Medical Device-Associated Infections Caused by Biofilm-Forming Microbial Pathogens and Controlling Strategies. *Antibiotics*. 2024 Jul 4;13(7):623. doi:10.3390/antibiotics13070623 View Article Online
DOI: 10.1039/D6LF00022C
- 1145
- 1146
- 1147 177. Prabhukhot GS, Eggleton CD, Kim M, Patel J. Impact of surface topography and hydrodynamic flow conditions on single and multispecies biofilm formation by *Escherichia coli* O157:H7 and *Listeria monocytogenes* in presence of promotor bacteria. *LWT*. 2024 Jun;201:116240. doi:10.1016/j.lwt.2024.116240
- 1148
- 1149
- 1150
- 1151 178. Xu L, Siedlecki CA. Submicron topography design for controlling staphylococcal bacterial adhesion and biofilm formation. *J Biomed Mater Res A*. 2022 Jun 7;110(6):1238–50. doi:10.1002/jbm.a.37369
- 1152
- 1153
- 1154 179. Zhou T, Wan X, Huang DZ, Li Z, Peng Z, Anandkumar A, et al. AI-aided geometric design of anti-infection catheters. *Sci Adv*. 2024 Jan 5;10(1). doi:10.1126/sciadv.adj1741
- 1155
- 1156 180. Ge X, Leng Y, Lu X, Ren F, Wang K, Ding Y, et al. Bacterial responses to periodic micropillar array. *J Biomed Mater Res A*. 2015 Jan;103(1):384–96. doi:10.1002/jbm.a.35182
- 1157
- 1158 181. Fadeeva E, Truong VK, Stiesch M, Chichkov BN, Crawford RJ, Wang J, et al. Bacterial Retention on Superhydrophobic Titanium Surfaces Fabricated by Femtosecond Laser Ablation. *Langmuir*. 2011 Mar 15;27(6):3012–9. doi:10.1021/la104607g
- 1159
- 1160
- 1161 182. Variola F, Francis-Zalzal S, Leduc A, Barbeau J, Nanci A. Oxidative nanopatterning of titanium generates mesoporous surfaces with antimicrobial properties. *Int J Nanomedicine*. 2014 May;2319. doi:10.2147/IJN.S61333
- 1162
- 1163
- 1164 183. Kim S, Jung UT, Kim SK, Lee JH, Choi HS, Kim CS, et al. Nanostructured Multifunctional Surface with Antireflective and Antimicrobial Characteristics. *ACS Appl Mater Interfaces*. 2015 Jan 14;7(1):326–31. doi:10.1021/am506254r
- 1165
- 1166
- 1167 184. Vadillo-Rodríguez V, Guerra-García-Mora AI, Perera-Costa D, González-Martín ML, Fernández-Calderón MC. Bacterial response to spatially organized microtopographic surface patterns with nanometer scale roughness. *Colloids Surf B Biointerfaces*. 2018 Sep;169:340–7. doi:10.1016/j.colsurfb.2018.05.038
- 1168
- 1169
- 1170
- 1171 185. Rostami S, Puza F, Ucak M, Ozgur E, Gul O, Ercan UK, et al. Bifunctional sharkskin mimicked chitosan/graphene oxide membranes: Reduced biofilm formation and improved cytocompatibility. *Appl Surf Sci*. 2021 Apr;544:148828. doi:10.1016/j.apsusc.2020.148828
- 1172
- 1173
- 1174 186. Serrano C, García-Fernández L, Fernández-Blázquez JP, Barbeck M, Ghanaati S, Unger R, et al. Nanostructured medical sutures with antibacterial properties. *Biomaterials*. 2015 Jun;52:291–300. doi:10.1016/j.biomaterials.2015.02.039
- 1175
- 1176
- 1177 187. Valle J, Burgui S, Langheinrich D, Gil C, Solano C, Toledo-Arana A, et al. Evaluation of Surface Microtopography Engineered by Direct Laser Interference for Bacterial Anti-Biofouling. *Macromol Biosci*. 2015 Aug;15(8):1060–9. doi:10.1002/mabi.201500107
- 1178
- 1179
- 1180 188. Elashnikov R, Ulbrich P, Vokatá B, Pavlíčková VS, Švorčík V, Lyutakov O, et al. Physically Switchable Antimicrobial Surfaces and Coatings: General Concept and Recent Achievements. *Nanomaterials*. 2021 Nov 16;11(11):3083. doi:10.3390/nano11113083
- 1181
- 1182
- 1183 189. Unepetty A, Dávila-Lezama A, Garibo D, Oknianska A, Bogdanchikova N, Hernández-Sánchez JF, et al. Strategies applied to modify structured and smooth surfaces: A step closer to reduce bacterial adhesion and biofilm formation. *Colloid Interface Sci Commun*. 2022;46:100560. doi:https://doi.org/10.1016/j.colcom.2021.100560
- 1184
- 1185
- 1186



- 1187 190. Zhang M, Yu Z, Lo ECM. A New pH-Responsive Nano Micelle for Enhancing the Effect of a
 1188 Hydrophobic Bactericidal Agent on Mature *Streptococcus mutans* Biofilm. *Front Microbiol.*
 1189 2021 Oct 18;12. doi:10.3389/fmicb.2021.761583
- 1190 191. Gu H, Lee SW, Carnicelli J, Zhang T, Ren D. Magnetically driven active topography for long-
 1191 term biofilm control. *Nat Commun.* 2020;11(1):2211. doi:10.1038/s41467-020-16055-5
- 1192 192. Oh MJ, Babeer A, Liu Y, Ren Z, Wu J, Issadore DA, et al. Surface Topography-Adaptive
 1193 Robotic Superstructures for Biofilm Removal and Pathogen Detection on Human Teeth. *ACS*
 1194 *Nano.* 2022 Aug 23;16(8):11998–2012. doi:10.1021/acsnano.2c01950
- 1195 193. Wang H, Zhang Z, Wang Z, Liang Y, Cui Z, Zhao J, et al. Multistimuli-Responsive
 1196 Microstructured Superamphiphobic Surfaces with Large-Range, Reversible Switchable
 1197 Wettability for Oil. *ACS Appl Mater Interfaces.* 2019 Aug 7;11(31):28478–86.
 1198 doi:10.1021/acsam.9b07941
- 1199 194. Elashnikov R, Lyutakov O, Ulbrich P, Svorcik V. Light-activated polymethylmethacrylate
 1200 nanofibers with antibacterial activity. *Materials Science and Engineering: C.* 2016 Jul;64:229–
 1201 35. doi:10.1016/j.msec.2016.03.047
- 1202 195. Yang C, Wu L, Li G. Magnetically Responsive Superhydrophobic Surface: In Situ Reversible
 1203 Switching of Water Droplet Wettability and Adhesion for Droplet Manipulation. *ACS Appl*
 1204 *Mater Interfaces.* 2018 Jun 13;10(23):20150–8. doi:10.1021/acsam.8b04190
- 1205 196. Děkanovský L, Elashnikov R, Kubiková M, Vokatá B, Švorčík V, Lyutakov O. Dual-Action
 1206 Flexible Antimicrobial Material: Switchable Self-Cleaning, Antifouling, and Smart Drug
 1207 Release. *Adv Funct Mater.* 2019 Aug 4;29(31). doi:10.1002/adfm.201901880
- 1208 197. Rajaramon S, David H, Sajeevan A, Shanmugam K, Sriramulu H, Dandela R, et al. Multi-
 1209 functional approach in the design of smart surfaces to mitigate bacterial infections: a review.
 1210 *Front Cell Infect Microbiol.* 2023 May 23;13. doi:10.3389/fcimb.2023.1139026
- 1211 198. Su Q, Xue Y, Wang C, Zhou Q, Zhao Y, Su J, et al. Strategies and applications of antibacterial
 1212 surface-modified biomaterials. *Bioact Mater.* 2025 Nov;53:114–40.
 1213 doi:10.1016/j.bioactmat.2025.07.009
- 1214 199. Perera-Costa D, Bruque JM, González-Martín ML, Gómez-García AC, Vardillo-Rodríguez V.
 1215 Studying the Influence of Surface Topography on Bacterial Adhesion using Spatially
 1216 Organized Microtopographic Surface Patterns. *Langmuir.* 2014 Apr 29;30(16):4633–41.
 1217 doi:10.1021/la5001057
- 1218 200. Jin E, Lv Z, Zhu Y, Zhang H, Li H. Nature-Inspired Micro/Nano-Structured Antibacterial
 1219 Surfaces. *Molecules.* 2024 Apr 23;29(9):1906. doi:10.3390/molecules29091906
- 1220 201. Thakur A, Ganesan R, Ray Dutta J. Nanomaterials against antimicrobial resistance and
 1221 beyond: toward mitigating bacterial resuscitation. *Total Environment Microbiology.* 2026
 1222 Mar;2(1):100052. doi:10.1016/j.temier.2025.100052
- 1223 202. Jagessar A, Shahali H, Mathew A, Yarlagadda PKD V. Bio-mimicking nano and micro-
 1224 structured surface fabrication for antibacterial properties in medical implants. *J*
 1225 *Nanobiotechnology.* 2017 Dec 2;15(1):64. doi:10.1186/s12951-017-0306-1
- 1226 203. Kaur R, Liu S. Antibacterial surface design – Contact kill. *Prog Surf Sci.* 2016 Aug;91(3):136–
 1227 53. doi:10.1016/j.progsurf.2016.09.001



- 1228 204. Soni A, Brightwell G. Nature-Inspired Antimicrobial Surfaces and Their Potential
1229 Applications in Food Industries. *Foods*. 2022 Mar 16;11(6):844. doi:10.3390/foods11060844 View Article Online
DOI: 10.1039/D6LF00022C
- 1230 205. Karimi K, Fardoost A, Mhatre N, Rajan J, Boisvert D, Javanmard M. A Thorough Review of
1231 Emerging Technologies in Micro- and Nanochannel Fabrication: Limitations, Applications,
1232 and Comparison. *Micromachines (Basel)*. 2024 Oct 21;15(10):1274. doi:10.3390/mi15101274
- 1233 206. Sen O, Poddar P, Sarkar P, Das S, Manna S. Current advancements in microneedle technology
1234 for therapeutic and biomedical applications. *Sensors International*. 2025;6:100325.
1235 doi:10.1016/j.sintl.2024.100325
- 1236 207. Sun Y, Yang Y, Jiang W, Bai H, Liu H, Wang J. In Vivo Antibacterial Efficacy of
1237 Nanopatterns on Titanium Implant Surface: A Systematic Review of the Literature.
1238 *Antibiotics*. 2021 Dec 14;10(12):1524. doi:10.3390/antibiotics10121524
- 1239 208. Lin N, Berton P, Moraes C, Rogers RD, Tufenkji N. Nanodarts, nanoblades, and nanospikes:
1240 Mechano-bactericidal nanostructures and where to find them. *Adv Colloid Interface Sci*. 2018
1241 Feb;252:55–68. doi:10.1016/j.cis.2017.12.007
- 1242 209. Abdelhamid AG, Yousef AE. Combating Bacterial Biofilms: Current and Emerging
1243 Antibiofilm Strategies for Treating Persistent Infections. *Antibiotics*. 2023 Jun 3;12(6):1005.
1244 doi:10.3390/antibiotics12061005
- 1245 210. Wang Y, Dong Y, Quan Y, Wackerow S, Abdolvand A, Zolotovskaya SA, et al. Hybrid
1246 Antibacterial Surfaces: Combining Laser-Induced Periodic Surface Structures with
1247 Polydopamine-Chitosan-Silver Nanoparticle Nanocomposite Coating. *Adv Mater Interfaces*.
1248 2025 Mar 17;12(6). doi:10.1002/admi.202400660
- 1249 211. Liu P, Wu Y, Tang K, Mehrjou B, Tao J, Wang G, et al. Enhanced antibacterial activity of
1250 polyphenol-bound microtopography by synergistic chemical and micro/nanomechanical
1251 effects. *Compos B Eng*. 2024 Jul;280:111498. doi:10.1016/j.compositesb.2024.111498
- 1252 212. Durand H, Whiteley A, Mailley P, Nonglaton G. Combining Topography and Chemistry to
1253 Produce Antibiofouling Surfaces: A Review. *ACS Appl Bio Mater*. 2022 Oct 17;5(10):4718–
1254 40. doi:10.1021/acsabm.2c00586
- 1255 213. Georgakopoulos-Soares I, Papazoglou EL, Karmiris-Obratański P, Karkalos NE, Markopoulos
1256 AP. Surface antibacterial properties enhanced through engineered textures and surface
1257 roughness: A review. *Colloids Surf B Biointerfaces*. 2023;231:113584.
1258 doi:https://doi.org/10.1016/j.colsurfb.2023.113584
- 1259 214. Koo H, Allan RN, Howlin RP, Stoodley P, Hall-Stoodley L. Targeting microbial biofilms:
1260 current and prospective therapeutic strategies. *Nat Rev Microbiol*. 2017 Dec 25;15(12):740–
1261 55. doi:10.1038/nrmicro.2017.99

1262

1263

